

---

# Robust covariance estimation with missing values and cell-wise contamination

---

**Karim Lounici**

CMAP

Ecole Polytechnique

Palaiseau, France

karim.lounici@polytechnique.edu

**Gregoire Pacreau**

CMAP

Ecole Polytechnique

Palaiseau, France

gregoire.pacreau@polytechnique.edu

## Abstract

Large datasets are often affected by cell-wise outliers in the form of missing or erroneous data. However, discarding any samples containing outliers may result in a dataset that is too small to accurately estimate the covariance matrix. Moreover, most robust procedures designed to address this problem are not effective on high-dimensional data as they rely crucially on invertibility of the covariance operator. In this paper, we propose an unbiased estimator for the covariance in the presence of missing values that does not require any imputation step and still achieves minimax statistical accuracy with the operator norm. We also advocate for its use in combination with cell-wise outlier detection methods to tackle cell-wise contamination in a high-dimensional and low-rank setting, where state-of-the-art methods may suffer from numerical instability and long computation times. To complement our theoretical findings, we conducted an experimental study which demonstrates the superiority of our approach over the state of the art both in low and high dimension settings.

## 1 Introduction

Outliers are a common occurrence in datasets, and they can significantly affect the accuracy of data analysis. While research on outlier detection and treatment has been ongoing since the 1960s, much of it has focused on cases where entire samples are outliers, as demonstrated by Huber's work [8, 30, 10]. While sample-wise contamination is a common issue in many datasets, modern data analysis often involves combining data from multiple sources. For example, data may be collected from an array of sensors, each with an independent probability of failure, or financial data may come from multiple companies, where reporting errors from one source do not necessarily impact the validity of the information from the other sources. Discarding an entire sample as an outlier when only a few features are contaminated can result in the loss of valuable information, especially in high-dimensional datasets where samples are already scarce. It is important to identify and address the specific contaminated features, rather than simply treating the entire sample as an outlier. In fact, if each dimension of a sample has a contamination probability of  $\epsilon$ , then the probability of that sample containing at least one outlier is given by  $1 - (1 - \epsilon)^p$ , where  $p$  is the dimensionality of the sample. In high dimension, this probability can quickly exceed 50%, surpassing the breakdown point of many

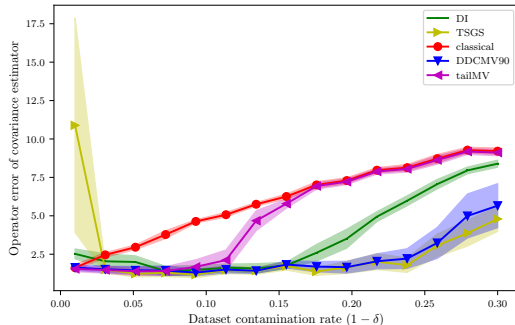


Figure 1: Left: Estimation error of the covariance matrix for  $n = 100$ ,  $p = 50$ ,  $\mathbf{r}(\Sigma) = 2$  under a Dirac contamination (tailMV and DDCMV are our methods). Here  $\epsilon = 1$  and  $\delta$  varies in  $(0, 1)$ . Right: For each method, mean computation time (in seconds) over 20 repetitions and whether it uses matrix inversion. For  $p = 100$ , we had to raise  $r(\Sigma)$  to 10 otherwise both DI and TSGS would fail due to numerical instability.

robust estimators designed for the Huber sample-wise contamination setting. Hence, it is crucial to develop robust methods that can handle cell-wise contaminations and still provide accurate results.

The issue of cell-wise contamination, where individual cells in a dataset may be contaminated, was first introduced in [2]. However, the issue of missing data due to outliers was studied much earlier, dating back to the work of [24]. Although missing values in a dataset are much easier to detect than outliers, they can still have a significant impact on the accuracy of statistical analysis and supervised learning tasks. Specifically, missing data can lead to errors in estimating the location and scale of the underlying distribution [16] and can negatively affect the performance of supervised learning algorithms [12]. Several robust estimation methods have been proposed to handle missing data, including Expectation Maximization (EM)-based algorithms [5], maximum likelihood estimation [11] and Multiple Imputation [16], among which we can find k-nearest neighbor imputation [28] and iterative imputation [31]. For the covariance matrix estimation in the Missing Completely At Random (MCAR) framework of [24], [17] provides suboptimal theoretical guarantees and a debiasing scheme for the estimation of the covariance.

In comparison to data missingness or its sample-wise counterpart, the cell-wise contamination problem is less studied. The Detection Imputation (DI) algorithm of [21] is an EM type procedure combining a robust covariance estimation method with an outlier detection method to iteratively update the covariance estimation. Other methods include adapting methodology created for Huber contamination for the cell-wise problem, such as in [4] or [1]. In high dimensional statistics, however, most of these methods fail due to high computation time and numerical instability. They are simply not designed to work in this regime since they are based on the Mahalanobis distance, which requires an inversion of the estimated covariance matrix. This is a major issue since classical covariance matrix estimators have many eigenvalues close to zero or even exactly equal to zero in high-dimension. Furthermore, to the best of our knowledge, no theoretical result exists concerning the statistical accuracy of these methods in the cell-wise contamination setting contrarily to the extensive literature on Huber’s contamination.

**Contributions.** In this paper, we address the problem of high-dimensional covariance estimation in the presence of missing observations and cell-wise contamination. To formalize this problem, we adopt and generalize the setting introduced in [7]. We propose a computationally efficient and numerically stable procedure that avoids matrix inversion, making it well-suited for high-dimensional data. We derive non-asymptotic estimation bounds of the covariance with the operator norm and matching minimax lower bounds (up to log), which clarify the impact of the missing value rate and outlier contamination rate. Our theoretical results also provide a significant improvement over [17] in the MCAR and no contamination setting. Next, we conduct an experimental study on synthetic data, comparing our proposed method to the state-of-the-art (SOTA) methods. Our results demonstrate that SOTA methods fail in the high-dimensional regime due to matrix inversions, while our proposed method performs well in this regime, highlighting its effectiveness. Then we demonstrate the practical

utility of our approach by applying it to real-life datasets, which highlights that the use of existing estimation methods significantly alters the spectral properties of the estimated covariance matrices. This implies that cell-wise contamination can significantly impact the results of dimension reduction techniques like principal component analysis (PCA) by completely altering the computed principal directions. Our experiments demonstrate that our method is more robust to cell-wise contamination than SOTA methods and produces reliable estimates of the covariance.

## 2 Missing values and cell-wise contamination setting

Let  $X_1, \dots, X_n$  be  $n$  i.i.d. copies of zero mean vector random vector  $X$  admitting unknown covariance operator  $\Sigma = \mathbb{E}[X \otimes X]$ , where  $\otimes$  is the outer product. Denote by  $X_i^{(j)}$  the  $j$ th component of vector  $X_i$  for any  $j \in [p]$ . All our results are non-asymptotic and cover all configurations of  $n, p$  including the high-dimensional setting  $p \gg n$ . In this paper, we consider the following two realistic scenarios where the measurements are potentially corrupted.

**Missing values.** We assume that each component  $X_i^{(j)}$  is observed independently from the others with probability  $\delta \in (0, 1]$ . Formally, we observe the random vector  $Y \in \mathbb{R}^p$  defined as follows:

$$Y_i^{(j)} = d_{i,j} X_i^{(j)}, 1 \leq i \leq n, 1 \leq j \leq p \quad (1)$$

where  $d_{i,j}$  are independent realisations of a bernoulli random variable of parameter  $\delta$ . This corresponds the Missing Completely at Random (MCAR) setting of [24].

**Cell-wise contamination.** Here we assume that some missing components  $X_i^{(j)}$  can be replaced with probability  $\varepsilon$  by some independent noise variables, representing either a poisoning of the data or random mistakes in measurements. The observation vector  $Y$  then satisfies:

$$Y_i^{(j)} = d_{i,j} X_i^{(j)} + (1 - d_{i,j}) e_{i,j} \xi_i^{(j)}, 1 \leq i \leq n, 1 \leq j \leq p \quad (2)$$

where  $\xi_1, \dots, \xi_n$  are i.i.d. erroneous measurements and  $e_{i,j}$  are i.i.d. bernoulli random variables with parameter  $\varepsilon$ . We also assume that all the variables  $X_i, \xi_i, d_{i,j}, e_{i,j}$  are mutually independent. In this scenario, a component  $X_i^{(j)}$  is either perfectly observed with probability  $\delta$ , replaced by a random noise with probability  $\varepsilon' = \varepsilon(1 - \delta)$  or missing with probability  $(1 - \delta)(1 - \varepsilon)$ . Cell-wise contamination as introduced in [2] corresponds to the case where  $\varepsilon = 1$ , and thus  $\varepsilon' = 1 - \delta$ .

If we consider the mean estimation problem, then the cell-wise contamination problem is indistinguishable from the classical Huber contamination problem since estimation of a mean vector is equivalent to the estimation of each marginal mean independently from the others. Since cell-wise contamination is equivalent to contamination of each marginal independently from the other marginals following Huber's paradigm, we can use for instance Tucker's median as a robust estimator of the mean. However, as argued in [2], the situation is quite different for covariance estimation.

Our proposal is based on a correction of the classical covariance estimator on  $Y_1, \dots, Y_n$  first introduced in [17] for the missing values scenario. The procedure is based on the following observation, with  $\Sigma^Y$  the covariance of the data with missing values and  $\Sigma$  the true covariance:

$$\Sigma = (\delta^{-1} - \delta^{-2}) \text{diag}(\Sigma^Y) + \delta^{-2} \Sigma^Y \quad (3)$$

Note that this formula assumes the knowledge of  $\delta$ . In the missing values scenario,  $\delta$  can be efficiently estimated by a simple count of the values exactly set to 0 or equal to NaN (not a number). However, in presence of contamination as in (2), one does not know the exact location and number of outliers. In our experiments, we will estimate  $\delta$  by the proportion of data remaining after a filtering procedure.

**Notations.** We denote by  $\odot$  the Hadamard (or term by term) product of two matrices and by  $\otimes$  the outer product of vectors, i.e.  $\forall x, y \in \mathbb{R}^d, x \otimes y = xy^\top$ . We denote by  $\|\cdot\|$  and  $\|\cdot\|_F$  the operator and Frobenius norms of a matrix respectively. The operator norm is defined as  $\|A\| = \sup\{\|Au\|_2, \|u\|_2 \leq 1\}$  with  $\|\cdot\|_2$  being the vector  $L_2$  norm.

### 3 Optimal estimation of covariance matrices with missing values

We consider the scenario outlined in (1) where the matrix  $\Sigma$  is of approximately low rank. To quantify this, we use the concept of effective rank, which provides a useful measure of the inherent complexity of a matrix. Specifically, the effective rank of  $\Sigma$  is defined as follows

$$\mathbf{r}(\Sigma) := \frac{\mathbb{E} \|X\|_2^2}{\|\Sigma\|} = \frac{\text{tr}(\Sigma)}{\|\Sigma\|} \quad (4)$$

We note that  $0 \leq \mathbf{r}(\Sigma) \leq \text{rank}(\Sigma)$ . Furthermore, for approximately low rank matrices with rapidly decaying eigenvalues, we have  $\mathbf{r}(\Sigma) \ll \text{rank}(\Sigma)$ . This section presents a novel analysis of the estimator defined in equation (3), which yields a non-asymptotic minimax optimal estimation bound in the operator norm. Our findings represent a substantial enhancement over the suboptimal guarantees reported in [17].

**Non-asymptotic upper-bound in the operator norm.** We provide an upper bound of the estimation error in operator norm. We write  $Y_i = d_i \odot X_i$ . Let  $\widehat{\Sigma}^Y = \sum_{i=1}^n Y_i \otimes Y_i / n$  be the classical covariance estimator of the covariance of  $Y$ . When the dataset contains missing values and corruptions,  $\widehat{\Sigma}^Y$  is a biased estimator of  $\Sigma$ . Exploiting (3), [17] proposed the following unbiased estimator of the covariance matrix  $\Sigma$ :

$$\widehat{\Sigma} = \delta^{-2} \widehat{\Sigma}^Y + (\delta^{-1} - \delta^{-2}) \text{diag}(\widehat{\Sigma}^Y). \quad (5)$$

**Theorem 1.** *Let  $X_1, \dots, X_n$  be i.i.d. subgaussian random variables in  $\mathbb{R}^p$ , with covariance matrix  $\Sigma$ , and let  $d_{ij}, i \in [1, n], j \in [1, p]$  be i.i.d. bernoulli random variables with probability of success  $\delta > 0$ . Then there exists an absolute constant  $C$  such that, for  $t > 0$ , with probability at least  $1 - e^{-t}$ :*

$$\|\widehat{\Sigma} - \Sigma\| \leq C \frac{\|\Sigma\|}{\delta} \left( \sqrt{\frac{\mathbf{r}(\Sigma)}{n}} \vee \frac{\mathbf{r}(\Sigma)}{n} \vee \sqrt{\frac{t}{n}} \vee \frac{t}{n} \right) \quad (6)$$

This bound improves upon [17, Proposition 3] which proved with probability at least  $1 - e^{-t}$ :

$$\|\widehat{\Sigma} - \Sigma\| \leq C \|\Sigma\| \left( \sqrt{\frac{\mathbf{r}(\Sigma)(t + \log(2p))}{\delta^2 n}} \vee \frac{\mathbf{r}(\Sigma)(t + \log(2p))}{\delta^2 n} (\delta + t + \log n) \right)$$

Contrarily to the previous display, the bound in (6) admits an improved dependence on the parameter  $\delta$  as we replaced  $\delta^2$  by  $\delta$  in the denominator. Actually, this bound is sharp minimax optimal as we will prove it in Theorem 2. The complete proof argument for Theorem 1 is provided in appendix E.2. It relies on a recent generic chaining result for quadratic processes. Comparatively, the bound in [17, Proposition 3] was based on non-commutative Bernstein inequality and is never minimax-optimal in any settings of  $\delta, n, p, \mathbf{r}(\Sigma)$ .

*Sketch of proof.* We note that the Schur-Horn theorem gives:  $\|\text{diag}(\widehat{\Sigma}^Y - \Sigma^Y)\| \leq \|\widehat{\Sigma}^Y - \Sigma^Y\|$  Which in turn leads to  $\|\widehat{\Sigma} - \Sigma\| \leq 2\delta^{-2} \|\widehat{\Sigma}^Y - \mathbb{E}[\widehat{\Sigma}^Y]\|$ . We bound  $\|\widehat{\Sigma}^Y - \mathbb{E}[\widehat{\Sigma}^Y]\|$  using a generic chaining argument.  $\square$

**Minimax lower-bound.** We now provide a minimax lower bound for the covariance estimation with missing values problem. Let  $\mathcal{S}_p$  the set of  $p \times p$  symmetric semi-positive matrices. Then, define  $\mathcal{C}_{\bar{r}} = \{S \in \mathcal{S}_p : \mathbf{r}(S) \leq \bar{r}\}$  the set of matrices of  $\mathcal{S}_p$  with effective rank at most  $\bar{r}$ .

**Theorem 2.** *Let  $p, n, \bar{r}$  be strictly positive integers such that  $p \geq \max\{n, 2\bar{r}\}$ . Let  $X_1, \dots, X_n$  be i.i.d. random vectors in  $\mathbb{R}^p$  with covariance matrix  $\Sigma \in \mathcal{C}_{\bar{r}}$ . Let  $(d_{i,j})_{1 \leq i \leq n, 1 \leq j \leq p}$  be an i.i.d. sequence of Bernoulli random variables with probability of success  $\delta \in (0, 1]$ , independent from the  $X_1, \dots, X_n$ . We observe  $n$  i.i.d. vectors  $Y_1, \dots, Y_n \in \mathbb{R}^p$  such that  $Y_i^{(j)} = d_{i,j} X_i^{(j)}$ ,  $i \in [n]$ ,  $j \in [p]$ . Then there exists two absolute constants  $C > 0$  and  $\beta \in (0, 1)$  such that:*

$$\inf_{\widehat{\Sigma}} \max_{\Sigma \in \mathcal{C}_{\bar{r}}} \mathbb{P}_{\Sigma} \left( \|\widehat{\Sigma} - \Sigma\| \geq C \frac{\|\Sigma\|}{\delta} \sqrt{\frac{\mathbf{r}(\Sigma)}{n}} \right) \geq \beta \quad (7)$$

where  $\inf_{\widehat{\Sigma}}$  represents the infimum over all estimators  $\widehat{\Sigma}$  of matrix  $\Sigma$  based on  $Y_1, \dots, Y_n$ .

This lower bound improves upon [17, Theorem 2] as it relaxes the hypotheses on  $n$  and  $\bar{r}$ . More specifically, the lower bound in [17] requires  $n \geq 2\bar{r}^2/\delta^2$  while we only need the mild assumption  $p \geq \max\{n, 2\bar{r}\}$ . Furthermore, the above lower bound matches the upper bound of Theorem 1 in the high-dimensional regime  $p \geq \max\{n, 2\bar{r}\}$  and  $n \geq \mathbf{r}(\Sigma)$ , hence clarifying the impact of missing data on the estimation rate via the parameter  $\delta$ .

Our proof argument leverages the properties of the Grassmann manifold, which has been previously utilized in different settings such as sparse PCA without missing values or contamination [33] and low-rank covariance estimation without missing values or contamination [14]. However, tackling missing values in the Grassmann approach is the main technical challenge as it modifies the distribution of observations and requires several additional nontrivial arguments to control the distribution divergences, which is a crucial step in deriving the minimax lower bound for our problem.

*Sketch of proof.* We first build a sufficiently large test set of hard-to-learn covariance operators exploiting entropy properties of the Grassmann manifold such that the distance between any two distinct covariance operator is at least of the order  $\frac{\|\Sigma\|}{\delta} \sqrt{\frac{\mathbf{r}(\Sigma)}{n}}$ . Next, in order to control the Kullback-Leibler divergence of the observations with missing values, we exploit in particular interlacing properties of eigenvalues of the perturbed covariance operators [26].  $\square$

**Heterogeneous missingness.** In the MCAR scenario, we assume now that each feature has a different missing value rate. We denote by  $\delta_j \in (0, 1]$  the probability to observe feature  $X^{(j)}$ ,  $1 \leq j \leq p$ . We define next  $\bar{\delta} = \max_j \{\delta_j\}$  and  $\underline{\delta} = \min_j \{\delta_j\}$  the largest and smallest probabilities to observe a feature. By a straightforward modification of  $\hat{\Sigma}$  and the proof of Theorem 1, under the same assumptions on  $X$ , we get, for any  $t > 0$ , with probability at least  $1 - e^{-t}$

$$\|\hat{\Sigma} - \Sigma\| \leq C \frac{\bar{\delta} \|\Sigma\|}{\underline{\delta}^2} \left( \sqrt{\frac{\mathbf{r}(\Sigma)}{n}} \vee \frac{\mathbf{r}(\Sigma)}{n} \vee \sqrt{\frac{t}{n}} \vee \frac{t}{n} \right). \quad (8)$$

Similarly we also obtain the following lower bound. For  $\delta \in [1/2, 1]$ , let  $p, n, \bar{r}$  be strictly positive integers such that  $n \geq 2\bar{r}/\delta^2$  and  $p \geq 2\bar{r}$ . Then we have

$$\inf_{\hat{\Sigma}} \max_{\Sigma \in \mathcal{C}_{\bar{r}}} \mathbb{P}_{\Sigma} \left( \|\hat{\Sigma} - \Sigma\| \geq C \|\Sigma\| \sqrt{\frac{\mathbf{r}(\Sigma)}{\delta^2 n}} \right) \geq \beta. \quad (9)$$

If  $\bar{\delta} \asymp \underline{\delta}$ , then the rates in (8) and (9) are matching and the minimax optimality result remains valid.

## 4 Optimal estimation of covariance matrices with cell-wise contamination

We consider the contamination scenario described in (2). We further assume that the  $\xi_1, \dots, \xi_n$  are subgaussian r.v. and that  $\Lambda := \mathbb{E}[\xi_1 \otimes \xi_1]$  is diagonal. In the presence of cell-wise contaminations, the operator  $\Sigma^Y = \mathbb{E}(Y \otimes Y)$  satisfies

$$\Sigma^Y = \delta^2 \Sigma + (\delta - \delta^2) \text{diag}(\Sigma) + \varepsilon(1 - \delta) \Lambda.$$

Note that the additional term  $\varepsilon(1 - \delta) \Lambda$  in the cell-wise contamination setting becomes negligible when  $\delta \approx 1$  or  $\varepsilon \approx 0$ . Using the DDC detection procedure of [21], we can detect the contaminations and accurately estimate both  $\delta, \varepsilon$  and the diagonal operator  $\Lambda$ . We will not develop this aspect further and simply assume that these are known in the following result. Hence we propose the following unbiased estimator of  $\Sigma$ . Let  $\hat{\Sigma}^Y = n^{-1} \sum_{i=1}^n Y_i \otimes Y_i$  and

$$\hat{\Sigma} = (\delta^{-1} - \delta^{-2}) \text{diag}(\hat{\Sigma}^Y) + \delta^{-2} \hat{\Sigma}^Y - \frac{\varepsilon(1 - \delta)}{\delta} \Lambda. \quad (10)$$

**Non-asymptotic upper-bound in the operator norm.** We prove the following result.

**Theorem 3.** *Let the assumptions of Theorem 1 be satisfied. We assume in addition that the observations  $Y_1, \dots, Y_n$  satisfy (2) with  $\varepsilon \in [0, 1)$  and  $\delta \in (0, 1]$ . Then, for any  $t > 0$ , with probability at*

least  $1 - e^{-t}$ :

$$\begin{aligned}
\|\widehat{\Sigma} - \Sigma\| &\lesssim \frac{\|\Sigma\|}{\delta} \left( \sqrt{\frac{\mathbf{r}(\Sigma)}{n}} \vee \frac{\mathbf{r}(\Sigma)}{n} \vee \sqrt{\frac{t}{n}} \vee \frac{t}{n} \right) \\
&\quad + \frac{\varepsilon(1-\delta)\|\Lambda\|}{\delta} \left( \sqrt{\frac{\mathbf{r}(\Lambda)}{n}} \vee \frac{\mathbf{r}(\Lambda)}{n} \vee \sqrt{\frac{t}{n}} \vee \frac{t}{n} \right) \\
&\quad + \left( \frac{1}{\delta} \sqrt{\varepsilon(1-\delta)} + \frac{\varepsilon(1-\delta)\sqrt{\delta}}{\delta^2} \right) \sqrt{\|\Lambda\| \|\Sigma\|} \sqrt{\mathbf{r}(\Lambda) \vee \mathbf{r}(\Sigma)} \sqrt{\frac{t + \log(\mathbf{r}(\Lambda) \vee \mathbf{r}(\Sigma))}{n}} \\
&\quad + \frac{\sqrt{\delta\varepsilon(1-\delta)}}{\delta^2} \sqrt{\|\Lambda\| \|\Sigma\|} \sqrt{\mathbf{r}(\Lambda) \vee \mathbf{r}(\Sigma)} \frac{(t + \log(\mathbf{r}(\Lambda) \vee \mathbf{r}(\Sigma))) \log n}{n}.
\end{aligned} \tag{11}$$

*Sketch of proof.* We first note that

$$\|\widehat{\Sigma} - \Sigma\| \leq \delta^{-2} \|\widehat{\Sigma}^Y - \Sigma^Y\| + \delta^{-2} \|\widehat{\Sigma}^{X,\xi,\delta,\varepsilon}\|. \tag{12}$$

The triangular inequality gives

$$\|\widehat{\Sigma}^Y - \Sigma^Y\| = \|\widehat{\Sigma}^\delta - \Sigma^\delta + \widehat{\Lambda}^\varepsilon - \mathbb{E}\widehat{\Lambda}^\varepsilon + \widehat{\Sigma}^{X,\xi,\delta,\varepsilon}\| \leq \|\widehat{\Sigma}^\delta - \Sigma^\delta\| + \|\widehat{\Lambda}^\varepsilon - \mathbb{E}\widehat{\Lambda}^\varepsilon\| + \|\widehat{\Sigma}^{X,\xi,\delta,\varepsilon}\|,$$

where the three empirical matrices are

1.  $\widehat{\Sigma}^\delta = n^{-1} \sum_{i=1}^n (d_i \otimes d_i) \odot (X_i \otimes X_i)$ , the empirical covariance matrix of the  $d_i \odot X_i$ ;
2.  $\widehat{\Lambda}^\varepsilon = n^{-1} \sum_{i=1}^n ((1-d_i) \odot e_i) \otimes ((1-d_i) \odot e_i) \odot (\xi_i \otimes \xi_i)$ , the empirical covariance of the  $(1-d_i) \odot e_i \odot \xi_i$  is such that  $\mathbb{E}\widehat{\Lambda}^\varepsilon = \frac{\varepsilon(1-\delta)}{\delta} \Lambda$ ;
3.  $\widehat{\Sigma}^{X,\xi,\delta,\varepsilon} = n^{-1} \sum_{i=1}^n (d_i \otimes [(1-d_i) \odot e_i]) \odot (X_i \otimes \xi_i) + (((1-d_i) \odot e_i] \odot d_i) \odot (\xi_i \otimes X_i)$  is the empirical covariance between the  $d_i \odot X_i$  and the  $(1-d_i) \odot e_i \odot \xi_i$ .

We tackle  $\|\widehat{\Sigma}^\delta - \Sigma^\delta\|$  and  $\|\widehat{\Lambda}^\varepsilon - \mathbb{E}\widehat{\Lambda}^\varepsilon\|$  similarly as in the proof of Thm 1. We tackle  $\|\widehat{\Sigma}^{X,\xi,\delta,\varepsilon}\|$  via a dimension-free non-commutative Bernstein inequality [18, 27]. See App E.3 for the full details.  $\square$

As emphasized in [13], the effective rank  $\mathbf{r}(\Sigma)$  provides a measure of the statistical complexity of the covariance learning problem in the absence of any contamination. However, when cell-wise contamination is present, the statistical complexity of the problem may increase if  $\mathbf{r}(\Lambda) \geq \mathbf{r}(\Sigma)$ . Fortunately, if the filtering process reduces the proportion of cell-wise contamination from  $\varepsilon$  to  $\varepsilon'$  such that  $\varepsilon' \text{tr}(\Lambda) \leq \text{tr}(\Sigma)$  and  $\varepsilon' \|\Lambda\| \leq \|\Sigma\|$ , then we can effectively mitigate the impact of cell-wise contamination, as highlighted in the following result.

**Corollary 1.** *Let the assumptions of Theorem 3 be satisfied. Assume in addition that  $\varepsilon \text{tr}(\Lambda) \leq \text{tr}(\Sigma)$  and  $\varepsilon \|\Lambda\| \leq \|\Sigma\|$ . Then, for any  $t > 0$ , with probability at least  $1 - e^{-t}$*

$$\begin{aligned}
\|\widehat{\Sigma} - \Sigma\| &\lesssim \frac{\|\Sigma\|}{\delta} \left( \sqrt{\frac{\mathbf{r}(\Sigma)}{n}} \vee \frac{\mathbf{r}(\Sigma)}{n} \vee \sqrt{\frac{t}{n}} \vee \frac{t}{n} \right) + \|\Sigma\| \frac{\varepsilon(1-\delta)}{\delta^2} \\
&\quad + \frac{\|\Sigma\| \mathbf{r}(\Sigma)}{\delta n} (1-\delta)(t + \log p) + \frac{\|\Sigma\|}{\delta} \sqrt{\frac{\mathbf{r}(\Sigma)}{n}} \frac{\sqrt{1-\delta} [t + \log p] \log n}{\sqrt{\delta n}}.
\end{aligned} \tag{13}$$

*Proof.* This is a straightforward consequence of Theorem 3.  $\square$

Table 1: Execution time of the covariance estimation procedures (in milliseconds) with  $n = 300$  averaged over all values of the contamination rate  $\delta$  and 20 repetitions.

method	$p = 50$	$p = 100$	$p = 500$
MV (ours)	$0.29 \pm 0.03$	$0.49 \pm 0.08$	$9.7 \pm 4.5$
KNNImputer (KNN)	$26 \pm 9.8$	$45 \pm 17$	$470 \pm 190$
IterativeImputer (II)	$940 \pm 350$	$2,800 \pm 900$	$1.7 \times 10^6 \pm 3.8 \times 10^5$

**Minimax lower-bound.** The lower bound for missing values still applies to the contaminated case as missing values are a particular case of contamination. However replacing missing values by adversarial contaminations and using the proof argument of [3] for Huber’s contamination, we obtain in the cell-wise setting the following minimax lower bound.

**Theorem 4.** *Let  $p, n, \bar{r}$  be strictly positive integers such that  $p \geq \max\{n, 2\bar{r}\}$ . Let  $X_1, \dots, X_n$  be i.i.d. random vectors in  $\mathbb{R}^p$  with covariance matrix  $\Sigma \in \mathcal{C}_{\bar{r}}$ . Let  $(d_{i,j})_{1 \leq i \leq n, 1 \leq j \leq p}$  be i.i.d. sequence of bernoulli random variables of probability of success  $\delta \in (0, 1]$ , independent to the  $X_1, \dots, X_n$ . We observe  $n$  i.i.d. vectors  $Y_1, \dots, Y_n \in \mathbb{R}^p$  satisfying (2) where  $\xi_i$  are i.i.d. of arbitrary distribution  $Q$ . Then there exists two absolute constants  $C > 0$  and  $\beta \in (0, 1)$  such that:*

$$\inf_{\hat{\Sigma}} \max_{\Sigma \in \mathcal{C}_{\bar{r}}} \max_Q \mathbb{P}_{\Sigma, Q} \left( \left\| \hat{\Sigma} - \Sigma \right\| \geq C \frac{\|\Sigma\|}{\delta} \sqrt{\frac{\mathbf{r}(\Sigma)}{n}} \sqrt{\epsilon(1-\delta)} \right) \geq \beta \quad (14)$$

where  $\inf_{\hat{\Sigma}}$  represents the infimum over all estimators of matrix  $\Sigma$  and  $\max_Q$  is the maximum over all contamination  $Q$ .

This lower bound combined with the upper bound of Corollary (1) clarifies the impact of the cell-wise contamination parameter  $\epsilon$ . The proof can be found in Appendix F.3.

## 5 Experiments

In our experiments, MV refers to the debiased covariance estimator (5). The synthetic data generation is described in Appendix A. We also performed experiments on real life datasets described in App. B. All experiments were conducted on a 2020 MacBook Air with a M1 processor (8 cores, 3.4 GHz).<sup>1</sup>

### 5.1 Missing Values

`sklearn` [20] provides two popular imputation methods: `KNNImputer`, which imputes the missing values based on the k-nearest neighbours [28], and `IterativeImputer`, which is inspired by the R package MICE [31]. In Figures 2, 3 and Table 1, we compare our estimator MV defined in (5) to these two imputation methods combined with the usual covariance estimator on synthetic data (see appendix A for details of data generation) in terms of statistical accuracy and execution time. We show that MV achieved a statistical accuracy similar to that of the SOTA `IterativeImputer` but is significantly faster even on moderately high dimensional data (less than 10 milliseconds for MV against about 28 minutes for `IterativeImputer`). MV also significantly beats `KNNImputer` both in term of statistical accuracy and computation time. We also see that trivial marginal imputation simply does not work. Based on these results, we can also argue that imputation of missing values is not mandatory for accurate estimation of the covariance operator : another viable option is to apply a debiasing correction to the empirical covariance computed on the original data containing missing values. The advantage of this approach is its low computational cost.

### 5.2 Cell-wise contamination

**Methods tested.** Our baselines are the empirical covariance estimator applied without care for contamination and an oracle which knows the position of every outlier, deletes them and then computes the MV bias correction procedure (5). In view of Theorems 1 and 2, this oracle procedure is the best possible in the setting of cell-wise contamination. Hence, we have a practical framework to assess the performance of any procedure designed to handle cell-wise contamination.

<sup>1</sup>Code available at <https://anonymous.4open.science/r/MVCE-C82F>

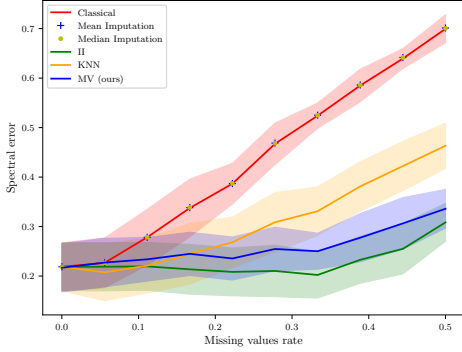


Figure 2: Estimation error on a synthetic dataset with  $p = 50$ ,  $n = 300$ ,  $r(\Sigma) = 5$ .

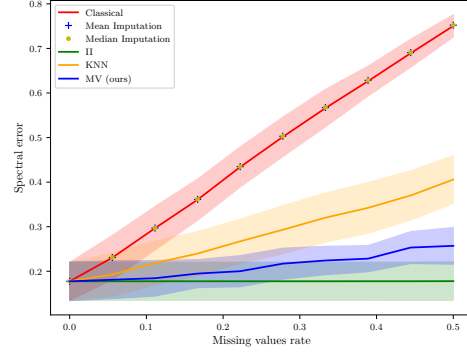


Figure 3: Estimation error on a synthetic dataset with  $p = 500$ ,  $n = 300$ ,  $r(\Sigma) = 5$ .

The SOTA methods in the cell-wise contamination setting are the `DI` (Detection-Imputation) method [21] and the `TSGS` method (Two Step Generalised S-estimator) [1]. Both these methods were designed to work in the standard setting  $n > p$  but cannot handle the high-dimensional setting as we already mentioned. Nevertheless, we included comparisons of our methods to them in the standard setting  $n > p$ . The code for `DI` and `TSGS` are from the R packages `cellwise` and `GSE` respectively.

Our estimators are referenced as `DDCMV` (short for Detecting Deviating Cells Missing Values), which uses the `DDC` detection procedure of [23] to first remove outliers and then compute the debiased covariance of (5) on the filtered data, and `tailMV`, which detects outliers through thresholding and then uses again (5). We also combined the filtering step with `KNNimpute` and `IterativeImputer` to define two additional novel robust procedures which we call `DDCKNN` and `DDCII`. To the best of our knowledge, this second alternative approach combining filtering with missing values imputation has never been tested to deal with cell-wise contamination. A detailed description of each method is provided in appendix C.

**Outlier detection and estimation error under cell-wise contamination on synthetic data.** We showed that the error of a covariance estimator under cell-wise contamination depends on the proportion of remaining outliers after a filtration. In table 2 we investigate the filtering power of the `Tail Cut` and `DDC` methods in presence of Dirac contamination. We consider the cell-wise contamination setting (2) in the most difficult case  $\epsilon = 1$  which means that an entry is either correctly observed or replaced by an outlier (in other words, the dataset does not contain any missing value). For each values of  $\delta$  in a grid, the quantities  $\hat{\delta}$  and  $\hat{\epsilon}$  are the proportions of true entries and remaining contaminations after filtering averaged over 20 repetitions. The `DDC` based methods are particularly efficient since the proportion of Dirac contamination drops from  $1 - \delta$  to virtually 0 for any  $\delta \geq 0.74$ . In Fig. 1 and 4, we see that the performance of our method is virtually the same as the oracle `OracleMV` as long as the filtering procedure correctly eliminates the Dirac contaminations. As soon as the filtering procedure fails, the statistical accuracy brutally collapses and our `DDC` based estimators no longer do better than the usual empirical covariance. In Table 6 in App. H and Fig. 5, we repeated the same experiment but with a centered Gaussian contamination. Contrarily to the Dirac contamination scenario, we see in Fig. 5 that the statistical accuracy of our `DDC` based methods slowly degrades as the contamination rate increases but their performance remains significantly better than that of the usual empirical covariance.

### 5.3 The effect of Cell-wise contamination on real-life datasets

We tested the methods on 8 datasets from `sklearn` and Woolridge’s book on econometrics [34]. These are low dimensional datasets (less than 20 features) representing various medical, social and economic phenomena. We also included 2 high-dimensional datasets. See App. B for the list of the datasets.

One interesting observation is that the instability of Mahalanobis distance-based algorithms is not limited to high-dimensional datasets. Even datasets with a relatively small number of features can exhibit instability. This can be seen in the performance of `DI` on the `Attend` dataset, as depicted in



Table 2: We consider contaminated data following model (2) contaminated with a Dirac contamination of high intensity with  $\epsilon = 1$  and for several values of  $\delta$  in a grid. For each  $\delta$ , we average the proportion of real data  $\hat{\delta}$  and contaminated data  $\hat{\epsilon}$  after filtering over 20 repetitions. Values are displayed in percentages ( $\hat{\delta}$  must be high,  $\hat{\epsilon}$  low)). STD stands for standard deviation.

CONTAMINATION RATE ( $1 - \delta$ )	TAIL CUT				DDC 99%				DDC 90%			
	$\hat{\delta}$	STD	$\hat{\epsilon}$	STD	$\hat{\delta}$	STD	$\hat{\epsilon}$	STD	$\hat{\delta}$	STD	$\hat{\epsilon}$	STD
0.1 %	99.6	0.023	0.000	0.000	99.1	0.029	0.000	0.000	94.8	0.054	0.00	0.00
1%	98.8	0.027	0.000	0.000	98.2	0.037	0.000	0.00	94.3	0.102	0.00	0.00
5%	94.9	0.013	0.000	0.000	94.6	0.018	0.000	0.000	91.8	0.060	0.00	0.000
10%	90.0	0.004	0.000	0.000	89.9	0.016	0.00	0.000	88.2	0.109	0.000	0.000
20%	80.0	0.000	20.0	0.000	80.0	0.003	0.017	0.035	79.4	0.035	0.009	0.022
30%	70.0	0.000	30.0	0.000	70.0	0.001	3.48	2.19	69.9	0.015	2.930	2.31

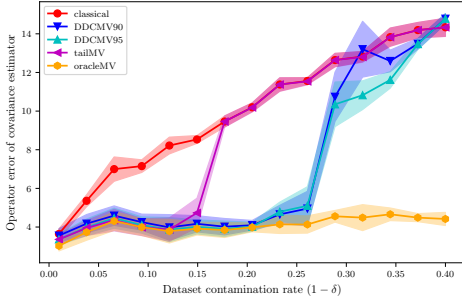


Figure 4: Estimation error as a function of the contamination rate for  $n = 500$ ,  $p = 400$ ,  $r(\Sigma) = 5$  and Dirac contamination .

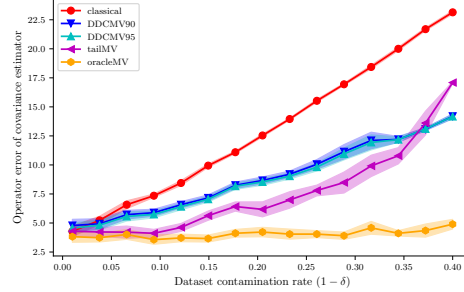


Figure 5: Estimation error as a function of the contamination rate for  $n = 500$ ,  $p = 400$ ,  $r(\Sigma) = 5$  and Gaussian contamination .

Figure 9, where it fails to provide accurate results. Similarly, both TSGS and DI fail to perform well on the CEOSAL2 dataset, as shown in Figure 11, despite both datasets having fewer than 15 features.

On the Abalone dataset, once we have removed 4 obvious outliers (which are detected by both DDC and the tail procedure), all estimators reached a consensus with the non-robust classical estimator, meaning that this dataset provides a ground truth against which we can evaluate and compare the performance of robust procedures in our study. To this end, we artificially contaminate 5% of the cells at random in the dataset with a Dirac contamination and compare the spectral error of the different robust estimators. As expected, TSGS and all our new procedures succeed at correcting the error, however DI becomes unstable (see Table 3). On Breast Cancer, DI also disagrees with every other procedures (see Figure 6), casting some doubt on the reliability of its estimate. We also performed experiments on 2 high-dimensional datasets, where our methods return stable estimates of the covariance (DDCMV99 and DDCMV95 are within  $\approx 3\%$  of each other) and farther away from the classical estimator (See Figures 13 and 14 in App. H). Note also that DDCII's computation time explodes and even returns out-of-memory errors due to the high computation cost of `IterativeImputer` that we already highlighted in Table 1.

## 6 Conclusion and future work

In this paper, we have derived sharp theoretical upper bounds on the spectral error of our covariance estimator robust to missing data with matching minimax lower bounds in the missing value setting. We have also derived the first theoretical guarantees in the cell-wise contamination setting. We highlighted in our numerical experimental study that in the missing value setting, our debiased estimator designed to tackle missing values without imputation offers statistical accuracy similar to the SOTA `IterativeImputer` for a dramatic computational gain. We also found that SOTA algorithms in the cell-wise contamination setting often fail in the standard setting  $p < n$  for dataset with fast decreasing eigenvalues (resulting in approximately low rank covariance), a setting which is commonly encountered in many real life applications. This is due to the fact that these methods use matrix inversion which is unstable to small eigenvalues in the covariance structure and can even fail

Table 3: Relative spectral difference (in percentages) between estimated covariance matrices on the Abalone data set with 5% synthetic contamination ( $\delta = 0.95$ ,  $\epsilon = 1$ ). On the cleaned dataset, all the robust estimators are very close to the empirical covariance (relative differences  $< 5\%$ ), so we consider its empirical covariance matrix as the truth. Notice that the DI procedure fails, probably due to numerical errors.

relative error to	Classical estimator	DDCMV99	DDCMV95	DDC KNN	DDC II	TSGS	DI
Truth	18.8	3.99	7.47	2.24	1.93	3.23	35.1
Classical	-	16.3	15.6	11.8	12.0	18.6	18.6
DDCMV99	-	-	3.79	7.05	7.25	5.75	34.1
DDCMV95	-	-	-	2.57	2.93	9.40	34.4
DDC KNN	-	-	-	-	0.40	4.06	34.2
DDC II	-	-	-	-	-	3.82	34.3
TSGS	-	-	-	-	-	-	34.3

to return any estimate. In contrast, we showed that our strategy combining filtering with estimation procedures designed to tackle missing values produce far more stable and reliable results. In future work, we plan to improve our theoretical upper and lower bounds in the cell-wise contamination setting to fully clarify the impact of this type of contamination in covariance estimation.

## References

- [1] Claudio Agostinelli, Andy Leung, Victor J. Yohai, and Ruben H. Zamar. Robust estimation of multivariate location and scatter in the presence of cellwise and casewise contamination, June 2014.
- [2] Fatemah Alqallaf, Stefan Van Aelst, Victor J. Yohai, and Ruben H. Zamar. Propagation of outliers in multivariate data. *The Annals of Statistics*, 37(1):311–331, February 2009.
- [3] Mengjie Chen, Chao Gao, and Zhao Ren. Robust Covariance and Scatter Matrix Estimation under Huber’s Contamination Model. *arXiv:1506.00691 [math, stat]*, June 2017.
- [4] Mike Danilov, Victor Yohai, and Ruben Zamar. Robust Estimation of Multivariate Location and Scatter in the Presence of Missing Data. *JASA. Journal of the American Statistical Association*, 107, September 2012.
- [5] A. P. Dempster, N. M. Laird, and D. B. Rubin. Maximum Likelihood from Incomplete Data via the EM Algorithm. *Journal of the Royal Statistical Society. Series B (Methodological)*, 39(1):1–38, 1977.
- [6] Sheela Devadas, Peter J. Haines, and Keaton Stubis. The schur-horn theorem. 2015.
- [7] Alessio Farcomeni. Robust Constrained Clustering in Presence of Entry-Wise Outliers. *Technometrics*, 56, February 2014.
- [8] Peter J. Huber. Robust Estimation of a Location Parameter. *The Annals of Mathematical Statistics*, 35(1):73–101, 1964.
- [9] Peter J. Huber and Elvezio M. Ronchetti. *Robust Statistics, 2nd Edition* | Wiley. Wiley Series in Probability and Statistics. John Wiley and Sons, Inc., 2009.
- [10] Mia Hubert, Michiel Debruyne, and Peter J. Rousseeuw. Minimum Covariance Determinant and Extensions. *WIREs Comp Stat*, 10(3), May 2018.
- [11] Mortaza Jamshidian and Peter M. Bentler. ML Estimation of Mean and Covariance Structures with Missing Data Using Complete Data Routines. *Journal of Educational and Behavioral Statistics*, 24(1):21–41, 1999.
- [12] Julie Josse, Nicolas Prost, Erwan Scornet, and Gaël Varoquaux. On the consistency of supervised learning with missing values. *arXiv:1902.06931 [cs, math, stat]*, July 2020.

- [13] Vladimir Koltchinskii and Karim Lounici. Concentration inequalities and moment bounds for sample covariance operators. *Bernoulli*, 23(1):110–133, February 2017.
- [14] Vladimir Koltchinskii, Karim Lounici, and Alexander B. Tsybakov. Estimation of Low-Rank Covariance Function, April 2015.
- [15] Andy Leung, Hongyang Zhang, and Ruben H. Zamar. Robust regression estimation and inference in the presence of cellwise and casewise contamination. *Computational Statistics & Data Analysis*, 99:1–11, July 2016.
- [16] Roderick Little and Donald Rubin. Statistical Analysis with Missing Data, Second Edition. Wiley Series in Probability and Mathematical Statistics. Probability and Mathematical Statistics. Wiley edition, 2002.
- [17] Karim Lounici. High-dimensional covariance matrix estimation with missing observations. *Bernoulli*, 20(3):1029–1058, August 2014.
- [18] Stanislav Minsker. On some extensions of bernstein’s inequality for self-adjoint operators. *arXiv: Probability*, 2011.
- [19] Alain Pajor. Metric Entropy of the Grassmann Manifold. *Complex Geometry Analysis*, 34:181–188, 1998.
- [20] F. Pedregosa, G. Varoquaux, A. Gramfort, V. Michel, B. Thirion, O. Grisel, M. Blondel, P. Prettenhofer, R. Weiss, V. Dubourg, J. Vanderplas, A. Passos, D. Cournapeau, M. Brucher, M. Perrot, and E. Duchesnay. Scikit-learn: Machine learning in Python. *Journal of Machine Learning Research*, 12:2825–2830, 2011.
- [21] Jakob Raymaekers and Peter J. Rousseeuw. Handling cellwise outliers by sparse regression and robust covariance. *arXiv:1912.12446 [stat]*, December 2020.
- [22] Jakob Raymaekers and Peter J. Rousseeuw. Fast robust correlation for high-dimensional data. *Technometrics*, 63(2):184–198, April 2021.
- [23] Peter J. Rousseeuw and Wannes Van den Bossche. Detecting deviating data cells. *Technometrics*, 60(2):135–145, April 2018.
- [24] Donald B. Rubin. Inference and Missing Data. *Biometrika*, 63(3):581–592, 1976.
- [25] Michel Talagrand. Majorizing measures: the generic chaining. *The Annals of Probability*, 24(3):1049 – 1103, 1996.
- [26] R. C. Thompson. Principal submatrices of normal and Hermitian matrices. *Illinois Journal of Mathematics*, 10(2):296–308, June 1966.
- [27] Joel A. Tropp. An introduction to matrix concentration inequalities. *Foundations and Trends® in Machine Learning*, 8(1-2):1–230, 2015.
- [28] Olga Troyanskaya, Michael Cantor, Gavin Sherlock, Pat Brown, Trevor Hastie, Robert Tibshirani, David Botstein, and Russ B. Altman. Missing value estimation methods for DNA microarrays. *Bioinformatics*, 17(6):520–525, June 2001.
- [29] Alexandre B. Tsybakov. Nonparametric estimators. In Alexandre B. Tsybakov, editor, *Introduction to Nonparametric Estimation*, Springer Series in Statistics, pages 1–76. Springer, New York, NY, 2009.
- [30] John W. Tukey. The Ninther, a Technique for Low-Effort Robust (Resistant) Location in Large Samples. In H. A. David, editor, *Contributions to Survey Sampling and Applied Statistics*, pages 251–257. Academic Press, January 1978.
- [31] Stef van Buuren and Karin Groothuis-Oudshoorn. Mice: Multivariate Imputation by Chained Equations in R. *Journal of Statistical Software*, 45:1–67, December 2011.
- [32] Roman Vershynin. Introduction to the non-asymptotic analysis of random matrices, November 2011.

- [33] Vincent Q. Vu and Jing Lei. Minimax sparse principal subspace estimation in high dimensions. *The Annals of Statistics*, 41(6):2905 – 2947, 2013.
- [34] Jeffrey M. Wooldridge. *Introductory econometrics : a modern approach*. Cengage learning, 2016.

Table 4: Notations

Symbol	Description
$X$	The random variable of interest
$Y$	The observed contaminated random variable
$p$	Dimension of the random variable
$n$	Number of samples
$\delta$	Probability that a cell be observed correctly
$\epsilon$	Probability that an unobserved cell be contaminated
$\Sigma$	True covariance matrix of $X$
$\Sigma^Y$	True covariance matrix of $Y$
$r(\Sigma)$	Effective rank of $\Sigma$
$\hat{\Sigma}$	Unbiased estimator of the covariance of $X$
$\hat{\Sigma}^Y$	Empirical covariance of $Y$
$\Lambda$	Noise covariance matrix
$\ X\ $	Operator norm of $X$
$\ X\ _F$	Forbenius norm of $X$
$\ X\ _{\psi_1}, \ X\ _{\psi_2}$	Orlicz norms of $X$
$\odot$	Hadamard or term by term product of matrices
$\otimes$	Outer product of vectors

Appendix A presents the synthetic data generation procedure used throughout our experiments. Appendix B and in particular Table 5 list the real life datasets presented in the paper. The cell-wise contamination correction methods are shown in Appendix C, with the DDC algorithm of [23] further detailed in Appendix D for convenience. The upper bound proofs can be found in Appendix E and the lower bound proofs in Appendix F, so that similar proof techniques be grouped together for clarity. Additional technical elements of these proofs were grouped in Appendix G when we felt that they impacted the latter’s readability. Finally, we show the full results of our experiments in Appendix H.

## A Synthetic data generation

We generate synthetic datasets of  $n$  realisations of a multivariate centered normal distribution. Its covariance matrix is defined as follows. We first set the eigenvalues as  $\exp(-j/r)$  for  $j \in \{1, p\}$ , where  $r$  is the requested effective rank of the matrix. This approximation guaranties that the true effective rank is below  $r+1$  for  $r \ll p$ . Then, using the `ortho-group` tool from `scipy.stats`, we create a random orthonormal matrix  $H$  and set  $\Sigma = H \text{diag}(g(\Lambda)) H^T$ , which is symmetric and of low effective rank at most  $r+1$ . Finally, we divide  $\Sigma$  by its largest diagonal term so that the variances of the marginals be closer to 1.

We contaminate our synthetic datasets using a binary mask obtained by computing the realisation of  $n \times p$  i.i.d. bernoulli random variables. We fill the resulting missing data with either  $n$  samples of a isotropic gaussian of covariance  $\sigma I_p$ , where  $\sigma$  is the strength of the contamination (which we call the Gaussian contamination) or a  $n \times p$  array of value  $\pm\sigma$  (which we call the Dirac contamination). Let  $\xi$  be a random vector following one of those two contaminations, the data we feed all algorithms is then  $Y = \text{mask} \odot X + (1 - \text{mask}) \odot \xi$ .

## B Real life data set

For our real data experiments, we removed any categorical variable from the datasets as well as variables that appeared to be mixtures of two distribution with different means. We also applied a log transform to skewed variables. The list of datasets can be found in Table 5. Finally, the Abalone dataset contains four obvious outliers that we removed in our experiments although they were easily detected by both DDC and the thresholding procedure.

Table 5: Datasets used in our real-life experiments.

Name	Source	$p$	$n$	$r(\Sigma)$	Description
Abalone	sklearn	7	4173	1.0	Characteristics of abalone specimens
Breast Cancer	sklearn	13	178	2.3	Data on cell nuclei
Wine	sklearn	30	69	2.8	Chemical data on wine varieties
Cameras	R	11	1038	2.7	Camera characteristics over different models
Attend	[34]	8	680	2.0	Class attendance
Barium	[34]	11	131	2.4	Barium exports
CEOSAL2	[34]	13	177	2.5	Firm accountancy data
INTDEF	[34]	12	49	2.2	USA deficit
SP 500	yfinance	496	502	2.7	Returns of SP 500 companies in 2021/2022
NASDAQ	yfinance	1442	502	4.0	Returns of NASDAQ companies in 2021/2022

## C Methods compared in the cell-wise contamination setting

### C.1 Baseline methods

**Classical** denotes the empirical covariance estimator applied without care for contamination. We expect all other methods to perform better than it.

**oracleMV** is an oracle that knows which cells are contaminated. This method shows the performance of our corrected estimator in the case of a perfect outlier detection algorithm, hence providing an idea of the optimal precision attainable with regard to the available information.

### C.2 Our methods

**tailMV** or tail Missing Values, is an estimator built by deleting extreme values in the dataset. It is actually one of the intermediary steps of DDC and we wanted to test how efficient it was on its own. We use the robust Huber estimator of the python package `Statsmodel.robust` [9] to compute the standard deviation of each marginal and eliminate any cell with value above 3 times these estimates.

**DDCMV** short for Detecting Deviating Cells Missing Values, is an estimator built using the DDC detection procedure of [21], where detected outliers are removed and considered as missing values. A detailed description of DDC is provided in appendix D. We then apply our corrected covariance estimator. We will add to the name of the method the quantile at which we consider a data as an outlier (DDCMV99 uses the 99-percentile of  $\chi_1^2$  for instance). When nothing is mentioned, assume that DDCMV99 is used. In our experiments, we use the R implementation found in the package `cellWise`, whose results are then sent to a python script for formatting.

**DDCKNN** detects outliers with the DDC procedure, removes them and imputes the missing values using the k-nearest neighbour procedure of [28] as implemented in sklearn under the name `KNNImputer`.

**DDCII** also detects and removes outliers with the DDC procedure, then imputes the missing values using sklearn’s `Iterative Imputer` class.

### C.3 SOTA methods for cell-wise contamination

**DI** or Detection Imputation [22] Is an iterative algorithm made of two alternating steps inspired by the Expectation Maximisation (EM) algorithm. The first detects outliers with regard to a previously estimated covariance matrix, then the second computes a new covariance matrix having removed the previously detected outliers using the M step of EM, but with bias correction. This new matrix is then the basis for the next detection step and so on. The authors found their algorithm to have a  $O(Tnp^3)$  complexity, with  $T$  the number of iterations, and make the assumption that the covariance matrix is of full rank to perform matrix inversion, both facts that make it difficult to use in high dimensions.

**TSGS** or Two Steps Generalised S-estimator [1] and [15] is also based on a two step process of detection then correction. Detection is based on the same DDC procedure while the estimation phase is based on the Generalised S-estimator of [4]. S-estimators are based on the Mahalanobis distance and thus require the true covariance matrix to be invertible. This may lead to numerical instability in our approximately low rank setting. However, if the matrix is of full rank, the generalised version of these estimators are proven to be consistent in the Missing Completely At Random setting.

## D The Detecting Deviating Cells algorithm

This section is entirely based on [23], whose algorithm we describe here for convenience. DDC (Detecting Deviating Cells) is a 7 steps algorithm. In the following, let  $(X_i^j)_{i \in [n], j \in [p]}$  be our dataset of  $n$  samples from data with dimension  $p$ .

**Step 1: standardisation** We start by assuming that the  $X_i$  follow a normal distribution and we set

$$Z_i^j = \frac{X_i^j - \mu_X^j}{\sigma_X^j}$$

with  $\mu_X^j$  being the empirical mean of marginal  $j$ , and  $\sigma_X^j$  its standard deviation.

**Step 2: cutoff** DDC sets to NA all values of  $Z_i^j$  if

$$|Z_i^j| \geq \sqrt{\chi_{1,p}^2}$$

with  $\chi_{1,p}^2$  the  $p^{\text{th}}$  centile of a  $\chi_1^2$  distribution, where  $p = 99\%$  by default.

**Step 3: bivariate relationship** The algorithm then computes the correlation between each couple of marginals. If  $|\rho_i(Z^j, Z^k)| \leq 0.5$ ; set  $b_{jk} = 0$ . Otherwise,

$$b_{jk} = \text{slope}(Z^j | Z^k)$$

with  $\text{slope}(x|y)$  the robust slope in the linear regression of  $x$  using  $y$ .

**Step 4: comparison** Then DDC tries to predict the expected values of each  $Z_i^j$  according to a weighted mean of the values of the other marginals, using the previously computed correlations as weights.

$$\hat{Z}_i^j = G(\{b_{jk} Z_i^k, k \in [p], k \neq j\})$$

with  $G$  the weighted mean using  $\rho(Z^j, Z^h)$  as weights.

**Step 5: deshrinkage** DDC adjusts the mean to account for shrinkage.

$$\begin{aligned} a_j &= \text{slope}(Z_i^j | \hat{Z}_i^j) \\ Z_i^{j*} &= a_j \hat{Z}_i^j \end{aligned}$$

**Step 6: residual computation** Then, one can take the residuals:

$$r_i^j = \frac{Z_i^j - \hat{Z}_i^j}{\mu_{Z^j - \hat{Z}^j}}$$

**Step 7: destandardisation** Finally, DDC returns the data to its actual location and scale. The residuals can then be tested using a  $\chi_1^2$  law to determine whether or not they are outliers.

## E Proof of upper bounds

### E.1 Tools and definitions

We recall the definition and some basic properties of sub-exponential random vectors.

**Definition 1.** For any  $\alpha \geq 1$ , the  $\psi_\alpha$ -norms of a real-valued random variable  $V$  are defined as:

$$\|V\|_{\psi_\alpha} = \inf\{u > 0, \mathbb{E} \exp(|V|^\alpha/u^\alpha) \leq 2\}$$

We say that a random variable  $V$  with values in  $\mathbb{R}$  is sub-exponential if  $\|V\|_{\psi_\alpha} < \infty$  for some  $\alpha \geq 1$ . If  $\alpha = 2$ , we say that  $V$  is sub-Gaussian. If a real-valued random variable  $V$  is sub-Gaussian, then  $V^2$  is sub-exponential. Indeed, we have:

$$\|V^2\|_{\psi_1} \leq 2 \|V\|_{\psi_2}^2$$

**Definition 2.** A random vector  $X \in \mathbb{R}^p$  is sub-exponential if  $\langle X, x \rangle$  are sub-exponential random variables for  $x \in \mathbb{R}^p$ . The  $\psi_\alpha$ -norms of a random vector  $X$  are defined as:

$$\|X\|_{\psi_\alpha} = \sup_{x \in \mathbb{R}^p, \|x\|_2=1} \|\langle X, x \rangle\|_{\psi_\alpha}, \quad \alpha \geq 1$$

We recall a version of Bernstein's inequality (see corollary 5.17 in [32]):

**Proposition 1.** Let  $Z_1, \dots, Z_n$  be independent sub-exponential zero mean real-valued random variables. Set  $K = \max_i \|Z_i\|_{\psi_1}$ . Then, for  $t > 0$ , with probability at least  $1 - e^{-t}$ :

$$\left| n^{-1} \sum_{i=1}^n Z_i \right| \leq CK \left( \sqrt{\frac{t}{n}} \vee \frac{t}{n} \right) \quad (15)$$

where  $C$  is an absolute constant.

## E.2 Proof of theorem 1

Let  $X_1, \dots, X_n$  be i.i.d. copies of random vector  $X$  satisfying

$$X = \sum_{k=1}^p \sqrt{\lambda_k} z_k \theta_k, \quad (16)$$

where  $\lambda_1 \geq \lambda_2 \geq \dots \geq \lambda_p \geq 0$ ,  $\{\theta_k\}_{k=1}^p$  is an orthonormal basis of  $\mathbb{R}^p$  and  $\{z_k\}_{k=1}^p$  is an i.i.d. sequence of subgaussian random variables. Without loss of generality, we assume that  $\|z_k\|_{\psi_2} = 1$ . In this framework,  $X$  admits covariance operator:

$$\Sigma = \sum_{k=1}^p \lambda_k \theta_k \otimes \theta_k.$$

Let for  $1 \leq i \leq n$  and  $1 \leq j \leq p$ ,  $d_{ij}$  follows an Bernoulli law  $\mathcal{B}(\delta)$ , with  $\delta \in [0, 1]$ , such that  $d_{ij}$  is independent both from  $X_i^{(j)}$ , that is the  $j$ th component of  $X_i$ , and of any other Bernoulli random variable. Let finally  $Y_i^{(h)} = d_{ij} X_i^{(j)}$  the observed random variable with missing values. We will denote by  $\lesssim$  the fact that the left side term is dominated by the right side term. This proof is the consequence of the following lemma:

**Lemma 1.** Under the same assumptions, let  $\Sigma^Y = \mathbb{E} Y \otimes Y$  and  $\widehat{\Sigma}^Y = n^{-1} \sum_{i=1}^n Y_i \otimes Y_i$ . There exist an absolute constant  $c_1$  such that, for  $t > 0$ , with probability at least  $1 - e^{-t}$ :

$$\left\| \widehat{\Sigma}^Y - \Sigma^Y \right\| \leq c_1 \delta \|\Sigma\| \left( \sqrt{\frac{\mathbf{r}(\Sigma)}{n}} \vee \frac{\mathbf{r}(\Sigma)}{n} \vee \sqrt{\frac{t}{n}} \vee \frac{t}{n} \right) \quad (17)$$

By definition of the operator norm, we can express this error in terms of Rayleigh's quotient:

$$\begin{aligned} \left\| n^{-1} \sum_i Y_i \otimes Y_i - \mathbb{E}[Y \otimes Y] \right\| &= \max_{\|u\|=1} u^\top \left( n^{-1} \sum_i Y_i \otimes Y_i - \mathbb{E}[Y \otimes Y] \right) u \\ &= \max_{\|u\|=1} n^{-1} \sum_i u^\top (Y_i \otimes Y_i) u^\top - u^\top \mathbb{E}[Y \otimes Y] u \\ &= \max_{\|u\|=1} n^{-1} \sum_i \langle d_i \odot X_i, u \rangle^2 - u^\top \mathbb{E}[Y \otimes Y] u. \end{aligned} \quad (18)$$



Let  $X$  and  $\tilde{\delta}$  be two random variables of same distribution to, respectively, the  $X_i$  and  $d_i$ . We can rewrite the expectation as:

$$u^\top \mathbb{E}[Y \otimes Y] u = \mathbb{E} u^\top (\tilde{\delta} \odot X) \otimes (\tilde{\delta} \odot X) u = \mathbb{E} \langle \tilde{\delta} \odot X, u \rangle^2 \quad (19)$$

Let  $\mathcal{F} = \{\langle \cdot, u \rangle, \|u\| \leq 1\}$ . Since  $X$  is subgaussian,  $\tilde{\delta} \odot X$  is too. This means that the  $\psi_1$  and  $\psi_2$  norms of linear functionals  $\langle \tilde{\delta} \odot X, u \rangle$  are both equivalent to the  $L_2$ -norm. Thus:

$$\sup_{f \in \mathcal{F}} \|f\|_{\psi_1} \lesssim \sup_{\|u\| \leq 1} \mathbb{E}^{1/2} \langle \tilde{\delta} \odot X, u \rangle^2 \leq \mathbb{E}^{1/2} \left\| \tilde{\delta} \odot X \right\|^2 = \mathbb{E}^{1/2} \sum_{i=1}^p \tilde{\delta}_i^2 X_i^2 \quad (20)$$

Since  $\tilde{\delta}$  is a Boolean vector,  $\forall i, \tilde{\delta}_i^2 = \tilde{\delta}_i$ . Thus, by the tower property:

$$\sup_{f \in \mathcal{F}} \|f\|_{\psi_1} \lesssim \mathbb{E}^{1/2} \mathbb{E}_{\tilde{\delta}} \sum_{i=1}^p \tilde{\delta}_i X_i^2 = \mathbb{E}^{1/2} \delta \|X\|^2 \leq \sqrt{\delta \|\Sigma\|}. \quad (21)$$

Now let us focus on  $\gamma_2(\mathcal{F}, \psi_2)$ . The norm equivalence and Talagrand's theorem [25] gives

$$\gamma_2(\mathcal{F}, \psi_2) \lesssim \gamma_2(\mathcal{F}, L_2) \lesssim \mathbb{E} \sup_{\|u\| \leq 1} \langle \tilde{\delta} \odot X, u \rangle \leq \sqrt{\delta \mathbb{E} \|X\|}. \quad (22)$$

Thus, under theorem 3 of [13], there exist an absolute constant  $c_1$  such that, for  $t > 0$ , with probability at least  $1 - e^{-t}$ :

$$\begin{aligned} \left\| \hat{\Sigma}^Y - \Sigma^Y \right\| &\lesssim \max \left\{ \sqrt{\delta} \|\Sigma\|^{1/2} \frac{\sqrt{\delta \mathbb{E} \|X\|}}{\sqrt{n}}, \frac{\delta \mathbb{E} \|X\|^2}{n}, \delta \|\Sigma\| \sqrt{\frac{t}{n}}, \delta \|\Sigma\| \frac{t}{n} \right\} \\ &= \delta \|\Sigma\| \left( \sqrt{\frac{\mathbf{r}(\Sigma)}{n}} \vee \frac{\mathbf{r}(\Sigma)}{n} \vee \sqrt{\frac{t}{n}} \vee \frac{t}{n} \right). \end{aligned} \quad (23)$$

Now note that  $\hat{\Sigma}^Y - \Sigma^Y$  is symmetric. By the Schur-Horn Theorem, we have that for any symmetric matrix  $A$ ,  $\max_i |A_{i,i}| \leq \|A\|$  (see e.g. [6] for the properties of the diagonal elements of Hermitian matrices and a demonstration of Schur-Horn theorem). In particular, this means that:

$$\left\| \text{diag} \left( \hat{\Sigma}^Y - \Sigma^Y \right) \right\| \leq \left\| \hat{\Sigma}^Y - \Sigma^Y \right\| \quad (24)$$

We are looking for an upper bound on:

$$\begin{aligned} \left\| \hat{\Sigma} - \Sigma \right\| &= \left\| (\delta^{-1} - \delta^{-2}) \text{diag} \left( \hat{\Sigma}^Y - \Sigma^Y \right) + \delta^{-2} \left( \hat{\Sigma}^Y - \Sigma^Y \right) \right\| \\ &\leq |\delta^{-1} - \delta^{-2}| \left\| \text{diag} \left( \hat{\Sigma}^Y - \Sigma^Y \right) \right\| + \delta^{-2} \left\| \hat{\Sigma}^Y - \Sigma^Y \right\| \\ &\leq \delta^{-2} \left\| \text{diag} \left( \hat{\Sigma}^Y - \Sigma^Y \right) \right\| + \delta^{-2} \left\| \hat{\Sigma}^Y - \Sigma^Y \right\|. \end{aligned} \quad (25)$$

Combining lemmas 1 and the argument on the diagonals with a union bound argument, and by reajusting the constants, we get that, for  $t > 0$ , with probability at least  $1 - e^{-t}$ :

$$\left\| \hat{\Sigma} - \Sigma \right\| \leq C \frac{\|\Sigma\|}{\delta} \left( \sqrt{\frac{\mathbf{r}(\Sigma)}{n}} \vee \frac{\mathbf{r}(\Sigma)}{n} \vee \sqrt{\frac{t}{n}} \vee \frac{t}{n} \right), \quad (26)$$

with  $C = 2c_1$  an absolute constant.

### E.3 Proof of the upper bound in the contaminated case

Using the previous result, we know that, with probability at least  $1 - e^{-t}$  and for an absolute constant  $C$ :

$$\left\| \hat{\Sigma}^\delta - \Sigma^\delta \right\| \leq C \frac{\|\Sigma\|}{\delta} \left( \sqrt{\frac{\mathbf{r}(\Sigma)}{n}} \vee \frac{\mathbf{r}(\Sigma)}{n} \vee \sqrt{\frac{t}{n}} \vee \frac{t}{n} \right), \quad (27)$$

and

$$\left\| \widehat{\Lambda}^\varepsilon - \mathbb{E} \widehat{\Lambda}^\varepsilon \right\| \leq C(1 - \delta)\varepsilon \|\Lambda\| \left( \sqrt{\frac{\mathbf{r}(\Lambda)}{n}} \vee \frac{\mathbf{r}(\Lambda)}{n} \sqrt{\frac{t}{n}} \vee \frac{t}{n} \right). \quad (28)$$

Now we need to control the norm of

$$\widehat{\Sigma}^{X, \xi, \delta, \varepsilon} = n^{-1} \sum_{i=1}^n (d_i \otimes [(1 - d_i) \odot e_i]) \odot (X_i \otimes \xi_i) + ([(1 - d_i) \odot e_i] \otimes d_i) \odot (\xi_i \otimes X_i).$$

To this end, we apply Theorem 7.3.1 in [27] in combination with a truncation argument as in [17] to obtain with probability at least  $1 - e^{-t}$

$$\begin{aligned} \left\| \widehat{\Sigma}^{X, \xi, \delta, \varepsilon} \right\| &\lesssim \left( \delta \sqrt{\varepsilon(1 - \delta)} + \varepsilon(1 - \delta) \sqrt{\delta} \right) \sqrt{\|\Lambda\| \|\Sigma\|} \sqrt{\mathbf{r}(\Lambda) \vee \mathbf{r}(\Sigma)} \sqrt{\frac{t + \log(\mathbf{r}(\Lambda) \vee \mathbf{r}(\Sigma))}{n}} \\ &\quad + \sqrt{\delta \varepsilon(1 - \delta)} \sqrt{\|\Lambda\| \|\Sigma\|} \sqrt{\mathbf{r}(\Lambda) \vee \mathbf{r}(\Sigma)} \frac{(t + \log(\mathbf{r}(\Lambda) \vee \mathbf{r}(\Sigma))) \log n}{n}. \end{aligned} \quad (29)$$

Notice next that  $\widehat{\Sigma}^{X, \xi, \delta, \varepsilon}$  has all its entries on the diagonal equal to zero. Hence applying the correction to obtain  $\widehat{\Sigma}$ , we get a control on  $\left\| \widehat{\Sigma}^{X, \xi, \delta, \varepsilon} \right\| / \delta^2$ .

Combining the last two displays with (12), (27) and (28) gives the result.

#### E.4 Adapting the proof to the heterogeneous missingness

Let  $\delta = (\delta_1, \dots, \delta_p)$  and  $\bar{\delta} = \max_j \delta_j$  and  $\underline{\delta} = \min_j \delta_j$ . It is quite obvious to see that equation 20 adapts as:

$$\sup_{f \in \mathcal{F}} \|f\|_{\psi_1} \lesssim \sqrt{\bar{\delta} \|\Sigma\|} \quad (30)$$

Similarly, equations 22 becomes:

$$\gamma_2(\mathcal{F}, \psi_2) \lesssim \sqrt{\bar{\delta} \|\Sigma\|} \quad (31)$$

and finally, we have that

$$\left\| \Delta \odot \left( \widehat{\Sigma}^Y - \Sigma^Y \right) \right\| \leq \underline{\delta}^{-2} \left\| \left( \widehat{\Sigma}^Y - \Sigma^Y \right) \right\| \quad (32)$$

## F Proof of lower bounds

The first two subsections deal with the lower bound of theorem 2, the third extends it to the contaminated case.

### F.1 Hypothesis construction in a Grassmannian manifold

Let  $p \geq 2$  be the dimension of our observations and let  $1 \leq r \leq p$  be the intrinsic dimension of  $\Sigma$ . Although the problem at hand is  $p$ -dimensional, we are most interested in correctly estimating the  $r$  eigenspaces related to the  $r$  largest eigenvalues. We will thus look at  $p$  dimensional matrices that are projection in  $\mathbb{R}^p$  of  $r$  dimensional kernels.

Let  $H$  be a  $p \times r$  matrix with orthonormal rows. Each matrix  $H$  describes a subspace  $U_H$  of  $\mathbb{R}^p$ , where  $\dim(U_H) = r$  and  $H^\top H$  is its projector in  $\mathbb{R}^p$ . The set of all  $U_H$  is the Grassmannian manifold  $G_r(\mathbb{R}^p)$ , which is the set of all  $r$ -dimensional subspaces of  $\mathbb{R}^p$ . The Grassmannian manifold is a smooth manifold of dimension  $d = r(p - r)$ , where one can define a metric for all subspaces  $U, \bar{U} \in G_r(\mathbb{R}^p)$ :

$$d(U, \bar{U}) = \|P_U - P_{\bar{U}}\|_F = \|H^\top H - \bar{H}^\top \bar{H}\| \quad (33)$$

where  $P_U$  and  $P_{\bar{U}}$  are the projectors to the subspaces  $U$  and  $\bar{U}$  respectively and  $H$  and  $\bar{H}$  are the  $r \times p$  matrix with orthonormal rows associated with  $U$  and  $\bar{U}$  respectively. In the remainder of the proof, we will identify the projectors to the subspaces. A result on the entropy of Grassmannian manifolds [19] shows that:

**Proposition 2.** For all  $\varepsilon > 0$ , there exists a family of orthonormal projectors  $\mathcal{U} \subset G_r(\mathbb{R}^p)$  such that:

$$|\mathcal{U}| \geq \left\lfloor \frac{\bar{c}}{\varepsilon} \right\rfloor^d \quad (34)$$

and,  $\forall P, Q \in G_r(\mathbb{R}^p), P \neq Q$ ,

$$\bar{c}\varepsilon\sqrt{r} \leq \|P - Q\|_F \leq \frac{\varepsilon\sqrt{r}}{\bar{c}} \quad (35)$$

for some small enough absolute constant  $\bar{c}$ , where  $|\mathcal{U}|$  is the cardinal of set  $\mathcal{U}$ .

Without loss of generality, we assume that the block matrix  $P_1 = \begin{pmatrix} I_r & 0 \\ 0 & 0 \end{pmatrix}$  belongs to the set  $\mathcal{U}$ .

Indeed, the Frobenius norm is invariant through a change of basis.

Let us then build such a set  $\mathcal{U}$  of hypotheses. Let  $\gamma = a\sqrt{p/\delta^2 n}$  where  $a > 0$  is an absolute constant. We set  $N = |\mathcal{U}|$  and  $\mathcal{U} = \{P_1, \dots, P_N\}$  where  $P_1$  was introduced above. Let us define the family of  $p \times p$  symmetric matrices  $\Sigma_1, \dots, \Sigma_N, \forall j \in \{1, N\}$  as follows :  $\Sigma_j = I_p + \gamma P_j$ , where  $I_p$  is the  $p \times p$  identity matrix. These covariance matrices belongs to the class of spiked covariance matrices.

Then, we can see that, for  $i, j \in \{1, \dots, N\}$ , by setting  $\varepsilon = 1/2$ :

$$\|\Sigma_i - \Sigma_j\|_F^2 = \gamma^2 \|P_i - P_j\|_F^2 > a^2 \bar{c}^2 \frac{pr}{2\delta^2 n} \quad (36)$$

## F.2 KL-divergence of hypotheses

Now that we have our candidate covariances  $\Sigma_1, \dots, \Sigma_N$ , let us define the associated distributions. For  $j \in \{1, N\}$ , let  $X_1, \dots, X_n$  be i.i.d. random variables following a gaussian  $\mathcal{N}(0, \Sigma_j)$  law. Let  $d_1, \dots, d_n$  be each vectors of  $p$  i.i.d bernoulli random variables of probability of success  $\delta > 0$ , and let  $Y_1, \dots, Y_n$  be random variables such that,  $\forall i \in \{1, n\}, Y_i = d_i \odot X_i$ , with  $\odot$  the Hadamard or term-by-term product. Let us also define as  $\mathbb{P}_j$  the distribution of  $Y_1, \dots, Y_n$  and  $\mathbb{P}_j^{(\delta)}$  the conditional distribution of the  $Y_1, \dots, Y_n$  knowing  $d_1, \dots, d_n$ . Finally, let  $\mathbb{E}_j$  be the expectation given the distribution associated with the  $j$ -th projector and  $\mathbb{E}_\delta$  the expectation given  $d_1, \dots, d_n$ .

For  $j \in \{2, \dots, N\}$ , let us compute the Kullback-Leibler divergence from  $\mathbb{P}_1$  to  $\mathbb{P}_j$ .

$$\begin{aligned} \text{KL}(\mathbb{P}_1, \mathbb{P}_j) &= \mathbb{E}_1 \log \left( \frac{d\mathbb{P}_1}{d\mathbb{P}_j} \right) = \mathbb{E}_1 \log \left( \frac{d\mathbb{P}_\delta \otimes \mathbb{P}_1^{(\delta)}}{d\mathbb{P}_\delta \otimes \mathbb{P}_j^{(\delta)}} \right) \\ &= \mathbb{E}_\delta \text{KL}(\mathbb{P}_1^{(\delta)}, \mathbb{P}_j^{(\delta)}) = \sum_{i=1}^n \mathbb{E}_\delta \text{KL}(\mathbb{P}_1^{(d_i)}, \mathbb{P}_j^{(d_i)}) \end{aligned} \quad (37)$$

Since  $\forall i \in \{1, \dots, n\}, Y_i | d_i \sim \mathcal{N}(0, (d_i \otimes d_i) \odot \Sigma)$ , for all  $j \in \{1, \dots, N\}$  and for each realisation  $\delta(\omega) \in \{0, 1\}^p, \mathbb{P}_j \gg \mathbb{P}_1$ , thus  $\text{KL}(\mathbb{P}_1, \mathbb{P}_j) < \infty$ .

Define  $J_i = \{j : d_{i,j} = 1, 1 \leq j \leq p\}$  the set of indices kept by vector  $d_i$  and  $p_i = \sum_{j=1}^p d_{i,j} \sim \mathcal{B}(p, \delta)$ . Then, define the mapping  $Q_i : \mathbb{R}^p \rightarrow \mathbb{R}^{d_i}$  such that  $Q_i(x) = x_{J_i}$ , such that  $x_{J_i}$  is a  $p_i$  dimensional vector containing the components of  $x$  whose index are in  $J_i$ . Let  $Q_i^* : \mathbb{R}^{d_i} \rightarrow \mathbb{R}^p$  the right inverse of  $Q_i$ .

Note that  $\forall j \in \{1, N-1\}, \Sigma_j = (1 + \gamma)P_j + P_j^\perp$ , with  $P_j^\perp$  the projector to the subspace of  $\mathbb{R}^p$  orthogonal to the one described by  $P_j$ . Let us define  $\Sigma_j^{(d_i)} = Q_i \Sigma_j Q_i^*$ . Then, observe that  $\Sigma_1^{(d_i)}$  is invertible, with inverse  $Q_i \left( \frac{1}{\gamma+1} P_1 + P_1^\perp \right) Q_i^*$  since  $P_1$  and  $P_1^\perp$  are diagonal matrices. We thus get, for  $i \in \{1, \dots, n\}$ :

$$\text{KL}(\mathbb{P}_1^{(d_i)}, \mathbb{P}_j^{(d_i)}) = \frac{1}{2} \left( \text{tr} \left( \Sigma_1^{(d_i)-1} \Sigma_j^{(d_i)} \right) - p_i - \log(\det(\Sigma_1^{(d_i)-1} \Sigma_j^{(d_i)})) \right) \quad (38)$$

First, using a result of linear algebra described in section G.2, we show that:

$$-\mathbb{E}_\delta \log(\det(\Sigma_1^{(d_i)-1} \Sigma_j^{(d_i)})) \leq ar\sqrt{p/n}. \quad (39)$$

In the high-dimensional regime  $p \geq n$ , we obtain

$$-n \mathbb{E}_\delta \log(\det(\Sigma_1^{(d_i)^{-1}} \Sigma_j^{(d_i)})) \leq ar\sqrt{np} \leq ar p. \quad (40)$$

Next, let us focus on bounding  $\frac{1}{2} \text{tr} \left( \Sigma_1^{(d_i)^{-1}} (\Sigma_j^{(d_i)} - \Sigma_1^{(d_i)}) \right)$ . Remember that  $\Sigma_1$  is diagonal. Using the fact that  $\Sigma_1^{-1} = \frac{1}{1+\gamma} P_1 + P_1^\perp$ , we get:

$$\begin{aligned} \text{tr} \left( \Sigma_1^{(d_i)^{-1}} (\Sigma_j^{(d_i)} - \Sigma_1^{(d_i)}) \right) &= \frac{\gamma}{1+\gamma} \text{tr} (Q_i P_1 (P_j - P_1) Q_i^*) + \gamma \text{tr} (Q_i P_1^\perp (P_j - P_1) Q_i^*) \\ &= \frac{\gamma}{1+\gamma} (\text{tr} (Q_i P_1 P_j Q_i^*) - \text{tr} (Q_i P_1 Q_i^*)) + \gamma \text{tr} (Q_i (I_p - P_1) P_j Q_i^*) \\ &= \left( \frac{\gamma}{1+\gamma} - \gamma \right) (\text{tr} (Q_i P_1 P_j Q_i^*) - p_i) \\ &= \frac{\gamma^2}{2(1+\gamma)} \|Q_i (P_j - P_1) Q_i^*\|_F^2 \end{aligned} \quad (41)$$

Finally, using the fact demonstrated in appendix G.4 and the upper bound of proposition 2, we get that:

$$\begin{aligned} \text{KL}(\mathbb{P}_1, \mathbb{P}_j) &\leq \sum_{i=1}^n \mathbb{E}_\delta \frac{\gamma^2}{2(1+\gamma)} \|Q_i (P_j - P_1) Q_i^*\|_F^2 \\ &\leq \sum_{i=1}^n \frac{\gamma^2 \delta}{2(1+\gamma)} \|P_j - P_1\|_F^2 \\ &\leq \sum_{i=1}^n \frac{\gamma \delta r}{8\bar{c}^2} \leq \frac{a}{8\bar{c}^2} r \sqrt{pn} \leq \frac{a^2}{4\bar{c}^2} r p. \end{aligned} \quad (42)$$

Thus, since  $N \geq \lfloor 2\bar{c} \rfloor^{r(p-r)}$ , and since we assumed that  $p > 2r$ :

$$\text{KL}(\mathbb{P}_1, \mathbb{P}_j) \leq \alpha \log(N) \quad (43)$$

for  $\alpha = a^2/8\bar{c}^2$ . According to theorem 2.5 of [29], the previous display combined with (36) gives

$$\inf_{\hat{\Sigma}} \sup_{\mathbb{P}_\Sigma} \mathbb{P}_\Sigma \left( \left\| \hat{\Sigma} - \Sigma \right\|_F^2 \geq C \frac{r}{\delta^2 n} p \right) \geq \beta \quad (44)$$

where  $C > 0$  and  $\beta > 0$  are two absolute constants. This fact, in turn, implies the lower bound of theorem 2, since, for all  $\Sigma_1, \Sigma_2$  matrices of our hypothesis set:

$$\|\Sigma_1 - \Sigma_2\|^2 \geq C \frac{r}{\delta^2 n} \quad (45)$$

Indeed, otherwise, we would get

$$\|\Sigma_1 - \Sigma_2\|_F^2 < p \|\Sigma_1 - \Sigma_2\|^2 < C \frac{r}{\delta^2 n} p \quad (46)$$

which contradicts equation 36.

### F.3 Lower bound in the contaminated case

The bound of theorem 4 is made of two terms. The left term is the missing values lower bound, since missingness is a particular case of contamination. The second term is a result from the Huber contamination analysis of [3], which we develop here.

Let us define the Huber contamination with missing values. Let  $P$  be a distribution and  $Q$  an arbitrary contamination distribuion. The Huber contaminated distribution  $\tilde{P}$  is defined as:

$$\tilde{P} = \delta P + \epsilon(1 - \delta)Q$$

where  $\delta, \epsilon \in [0, 1]$ . Let  $P$  be a parametric distribution  $P_\theta$ , whose parameter  $\theta \in \Theta$  we want to estimate.

Theorem 5.1 in [3] states that for two parametric distributions  $P_{\theta_1}$  and  $P_{\theta_2}$  with parameters  $\theta_1, \theta_2 \in \Theta$  respectively, there exist two contaminations  $Q_1$  and  $Q_2$  such that  $\tilde{P}_1$  and  $\tilde{P}_2$  are not identifiable, as long as the parameter distance  $L(\theta_1, \theta_2)$  is below the modulus of continuity:

$$\omega(\epsilon(1-\delta), \Theta) = \sup \left\{ L(\theta_1, \theta_2) : \text{TV}(\mathbb{P}_{\theta_1}, \mathbb{P}_{\theta_2}) \leq \frac{\epsilon(1-\delta)}{\delta}, \theta_1, \theta_2 \in \Theta \right\}$$

This formulation is slightly different than the one in [3] to account for missingness without contamination.

In appendix E, [3] gives a lower bound to this value in the case where  $\theta$  is a covariance matrix. Let  $\Sigma_1 = \mathbb{I}_p$  and  $\Sigma_2 = \mathbb{I}_p + \epsilon(1-\delta)E_{1,1}$ , where  $E_{1,1}$  is the matrix with zeros except in the  $(1, 1)$  entry, which is equal to 1. Then, set  $P_1 = \mathcal{N}(0, \Sigma_1)$  and  $P_2 = \mathcal{N}(0, \Sigma_2)$ . Observe that:

$$\text{TV}(P_1, P_2) \leq \frac{1}{2} \text{KL}(P_1, P_2) \leq \frac{1}{8} \|P_1 - P_2\|_F^2 = \frac{(\epsilon(1-\delta))^2}{8}$$

and

$$L(\Sigma_1, \Sigma_2) = \|\Sigma_1 - \Sigma_2\|^2 = (\epsilon(1-\delta))^2$$

Thus  $\omega(\epsilon(1-\delta), \Theta) > (\epsilon(1-\delta))^2$ . They conclude using Le Cam's two point method (see e.g. chapter 2.3 of [29]) that there exist two absolute constants  $C, c > 0$  such that:

$$\inf_{\hat{\Sigma}} \sup_{\Sigma} \sup_Q \tilde{P} \left( \left\| \hat{\Sigma} - \Sigma \right\| \geq C\epsilon(1-\delta) \right) > c$$

This is for Huber contamination. Let us now examine what happens for cell-wise contamination using the same hypotheses  $P_1$  and  $P_2$ . Note  $\tilde{P}_1$  and  $\tilde{P}_2$  the distributions of  $P_1$  and  $P_2$  cell-wise contaminated by two distributions  $Q_1$  and  $Q_2$  that we will both set with independent components. Since  $P_1$  and  $P_2$  are isotropic Gaussians and the contamination is completely at random, we can decompose the distributions as follows:

$$\tilde{P}_1 = \prod_{i=1}^p \delta P_{1,i} + \epsilon(1-\delta)Q_{1,i}$$

and

$$\tilde{P}_2 = \prod_{i=1}^p \delta P_{2,i} + \epsilon(1-\delta)Q_{2,i}$$

Notice that taken separately, the components can be considered to be univariate Gaussian distributions under a Huber contamination. We can now try to build  $Q_1$  and  $Q_2$  so that  $\tilde{P}_1$  and  $\tilde{P}_2$  are equal in distribution. Let us first set  $Q_{1,i} = Q_{2,i} = \mathcal{N}(0, 1)$  for  $i \neq 1$ , since the components are equal in distribution for  $i \neq 1$  the contamination we choose here doesn't matter much. As  $\omega(\epsilon(1-\delta), \Theta) > (\epsilon(1-\delta))^2$ , using the construction of theorem 5.1 in [3], we can build two distributions  $q_1$  and  $q_2$  such that:

$$\delta P_{1,1} + \epsilon(1-\delta)q_1 = \delta P_{2,1} + \epsilon(1-\delta)q_2$$

Let us thus set  $Q_{1,1} = q_1$  and  $Q_{2,1} = q_2$ . Under this contamination, we have  $\tilde{P}_1 = \tilde{P}_2$ . By applying Le Cam's two point argument, we find here again that there exist two absolute constants  $C, c > 0$  such that:

$$\inf_{\hat{\Sigma}} \sup_{\Sigma} \sup_Q \tilde{P} \left( \left\| \Sigma - \hat{\Sigma} \right\| > C\epsilon(1-\delta) \right) > c$$

## G Other proofs

### G.1 Proof of the correction formula of equation 10

Let  $X$  be a zero mean random vector of  $\mathbb{R}^p$  admitting covariance matrix  $\Sigma$ . Let  $\xi$  be a zero mean random vector, independent from  $X$ , with diagonal covariance matrix  $\Lambda$ . Let  $(d_j)_{1 \leq j \leq p}$

and  $(e_j)_{1 \leq j \leq p}$  sequences of Bernoulli random variables of probability respectively  $\delta$  and  $\varepsilon(1 - \delta)$ , independent from both  $X$  and  $\xi$  and such that  $1 \leq j \leq p, d_j e_j = 0$ . Then, let  $Y_i^{(j)} = d_j \odot X^{(j)} + e_j \odot \xi^{(j)}$ . We have that:

$$(Y \otimes Y)_{jk} = \begin{cases} d_j (X^{(j)})^2 + e_j (\xi^{(j)})^2 & \text{if } j = k \\ d_j d_k X^{(j)} X^{(k)} + d_j e_k X^{(j)} \xi^{(k)} + e_j d_k \xi^{(j)} X^{(k)} + e_j e_k \xi^{(j)} \xi^{(k)} & \text{otherwise} \end{cases} \quad (47)$$

This means that we have, by independence of the  $X^{(j)}$  and the  $\xi^{(j)}$ , and by independence of the  $\xi^{(j)}$  with each other:

$$\Sigma_{jk}^Y = \mathbb{E}(Y \otimes Y)_{jk} = \begin{cases} \delta \Sigma_{jj} + \varepsilon(1 - \delta) \Lambda_{jj} & \text{if } j = k \\ \delta^2 \Sigma_{jk} & \text{otherwise} \end{cases} \quad (48)$$

Thus:

$$\Sigma_{jk} = \begin{cases} \delta^{-1} (\Sigma_{jj}^Y - \varepsilon(1 - \delta) \Lambda_{jj}) & \text{if } j = k \\ \delta^{-2} \Sigma_{jk}^Y & \text{otherwise} \end{cases} \quad (49)$$

Which in turn means that:

$$\Sigma = (\delta^{-1} - \delta^{-2}) \text{diag}(\Sigma^Y) + \delta^{-2} \Sigma^Y + \frac{\varepsilon(1 - \delta)}{\delta} \Lambda \quad (50)$$

This gives the general correction formula with independent contamination. For the missing values correction, simply set  $\Lambda = \mathbf{0}$  the  $p \times p$  zero matrix.

## G.2 Bounds on the determinant of in equation 40

Theorem 13 of [26] states that, for any matrix  $A$  of size  $p$  with eigenvalues  $\lambda_1, \dots, \lambda_s$ , each with multiplicity  $\mu_1, \dots, \mu_s$  such that  $\sum_{i=1}^s \mu_i = p$ , then any principal submatrix  $A(j|j)$ , that is, a matrix created by removing line  $j$  and column  $j$  from  $A$ , has eigenvalues  $\lambda_i$  with multiplicity  $\max(0, \mu_i - 1)$ . The remaining eigenvalues have values between  $\min_i \lambda_i$  and  $\max_i \lambda_i$ .

In our case, the matrix  $\Sigma_j$  has only two eigenvalues:  $1 + \gamma$  and  $1$ , with multiplicity  $r$  and  $p - r$  respectively. One will easily find by recurrence on the number of deleted dimensions, which is  $p - p_i$  with  $p_i = \sum_{j=1}^p d_{i,j}$ , that:

$$\det \Sigma_j^{(d_i)} = (1 + \gamma)^{\max(0, r - p + p_i)} \prod_{k=1}^{p - p_i} \lambda_k \quad (51)$$

where  $\forall k \in \{1, p_i\}, 1 \leq \lambda_k \leq 1 + \gamma$ .

This means, in particular, that:

$$(1 + \gamma)^{\max(0, r - p + p_i)} \leq \det \Sigma_j^{(p_i)} \leq (1 + \gamma)^{\min(r, p_i)} \quad (52)$$

Now, let us demonstrate the statement in equation 40. We have  $\Sigma_1$  and  $\Sigma_j$  having the same eigenvalues  $1 + \gamma$  and  $1$  with multiplicity respectively  $r$  and  $p - r$ . Let  $p_i = \sum_{k=1}^p d_{i,k}$  be the number of remaining components after applying the boolean filter  $d_i$  (thus there are  $p - p_i$  deleted components). Since  $\Sigma_1$  is diagonal, we know that  $\Sigma_1^{(d_i)}$  will also have eigenvalues  $1 + \gamma$  and  $1$ , with multiplicity  $a_i$  and  $b_i$  respectively, where  $a_i \sim \mathcal{B}(r, \delta)$  and  $b_i \sim \mathcal{B}(p - r, \delta)$  where  $\mathcal{B}$  is the binomial distribution.

Then, using the lower bound we just demonstrated, we get that:

$$\begin{aligned} -\mathbb{E}_\delta \log \left( \det \left( \Sigma_1^{(d_i)-1} \Sigma_j^{(d_i)} \right) \right) &= \mathbb{E}_\delta a_i \log(1 + \gamma) + b_i \log(1) - \log \left( \det \left( \Sigma_j^{(d_i)} \right) \right) \\ &\leq \mathbb{E}_\delta a_i \log(1 + \gamma) - \max(0, r - p + p_i) \log(1 + \gamma) \\ &\leq (r\delta + \min(0, p - p_i - r)) \log(1 + \gamma) \\ &\leq r\delta \log(1 + \gamma) \end{aligned} \quad (53)$$

In particular, we know that  $\gamma > 0$ , so  $\log(1 + \gamma) \leq \gamma$  and

$$-\mathbb{E}_\delta \log \left( \det \left( \Sigma_1^{(d_i)-1} \Sigma_j^{(d_i)} \right) \right) \leq r\delta\gamma \leq a r \sqrt{p/n}. \quad (54)$$

### G.3 Behaviour of the $Q_i$ with regard to matrix multiplication

We know that  $Q_i Q_i^* = I_{d_i}$ . Furthermore,  $Q_i^* Q_i = I_p^{(j_i)}$ , where  $I_p^{(j_i)}$  is the diagonal matrix where the  $j$ th diagonal term is 1 if only if  $j \in J_i$ , and 0 otherwise.

Finally, notice that in the general case,  $Q_i A Q_i^* Q_i B Q_i^* \neq Q_i A B Q_i^*$ , except when either  $A$  or  $B$  is diagonal. Indeed, for  $k, l \in \{1, p\}$ :

$$(Q_i A Q_i^* Q_i B Q_i^*)_{kl} = \sum_{m=1}^p A_{km} B_{ml} \mathbb{1}_{k \in J_i} \mathbb{1}_{l \in J_i} \mathbb{1}_{m \in J_i} \quad (55)$$

Which, if  $A$  is diagonal, simply gives:

$$\begin{aligned} (Q_i A Q_i^* Q_i B Q_i^*)_{kl} &= A_{kk} B_{kl} \mathbb{1}_{k \in J_i} \mathbb{1}_{l \in J_i} \\ &= (Q_i A B Q_i^*)_{kl} \end{aligned} \quad (56)$$

### G.4 Proof of the upper bound of the frobenius norm with missing values

Let  $P \in \mathbb{R}^{p \times p}$  be any matrix, then, using the fact that the  $d_i$  are boolean vectors:

$$\begin{aligned} \mathbb{E}_\delta \| (d_i \otimes d_i) \odot P \|_F^2 &= \mathbb{E}_\delta \text{tr} \left( ((d_i \otimes d_i) \odot P)^\top ((d_i \otimes d_i) \odot P) \right) \\ &= \mathbb{E}_\delta \sum_{k=1}^p \sum_{l=1}^p d_i^k d_i^l P_{kl}^2 \\ &= \sum_{k=1}^p \left( \delta P_{kk} + \sum_{\substack{l=1 \\ l \neq k}}^p \delta^2 P_{kl}^2 \right) \\ &\leq \delta \|P\|_F^2 \end{aligned} \quad (57)$$

## H Tables

Table 6: We consider the cell-wise contamination model ((2)) with a Gaussian contamination of high intensity,  $\varepsilon = 1$  and for several values of  $\delta$  in a grid. For each  $\delta$ , we average the proportion of real data  $\hat{\delta}$  and contaminated data  $\hat{\varepsilon}$  after filtering over 20 repetitions. Values are displayed in percentages ( $\hat{\delta}$  must be high,  $\hat{\varepsilon}$  low, both are expressed in percentages).

CONTAMINATION RATE	TAIL CUT				DDC 99%				DDC 90%			
	$\hat{\delta}$	STD	$\hat{\varepsilon}$	STD	$\hat{\delta}$	STD	$\hat{\varepsilon}$	STD	$\hat{\delta}$	STD	$\hat{\varepsilon}$	STD
0.1%	99.6	0.025	0.034	0.003	99.0	0.033	0.055	0.003	94.8	0.091	0.053	0.003
1%	98.8	0.025	0.372	0.022	98.2	0.040	0.597	0.015	94.1	0.058	0.565	0.016
5%	94.9	0.011	1.87	0.157	94.5	0.035	3.01	0.055	91.1	0.090	2.84	0.046
10%	89.9	0.008	3.99	0.277	89.6	0.017	6.19	0.093	87.1	0.052	5.80	0.064
20%	80.0	0.003	9.69	0.239	79.7	0.028	13.8	0.113	78.4	0.072	12.6	0.104
30%	70.0	0.000	17.1	0.705	70.0	0.001	22.1	0.387	69.6	0.038	19.7	0.275

Table 7: Same table on the Abalone dataset, contaminated with a Dirac contamination.

CONTAMINATION RATE	TAIL CUT				DDC 99%				DDC 90%			
	$\hat{\delta}$	STD	$\hat{\varepsilon}$	STD	$\hat{\delta}$	STD	$\hat{\varepsilon}$	STD	$\hat{\delta}$	STD	$\hat{\varepsilon}$	STD
0.1%	69.5	0.001	0.000	0.000	98.0	0.010	0.000	0.000	93.2	0.020	0.000	0.000
1%	68.9	0.005	0.000	0.000	97.2	0.023	0.000	0.000	92.6	0.039	0.000	0.000
5%	66.2	0.034	0.000	0.000	93.6	0.043	0.000	0.000	89.8	0.083	0.000	0.000
10%	62.8	0.016	0.000	0.000	89.0	0.034	0.000	0.000	86.0	0.045	0.000	0.000
20%	56.0	0.002	6.00	0.000	79.9	0.070	0.138	0.163	79.6	0.355	0.001	0.003
30%	49.0	0.000	9.00	0.000	70.0	0.000	29.5	0.036	70.0	0.000	24.2	0.127

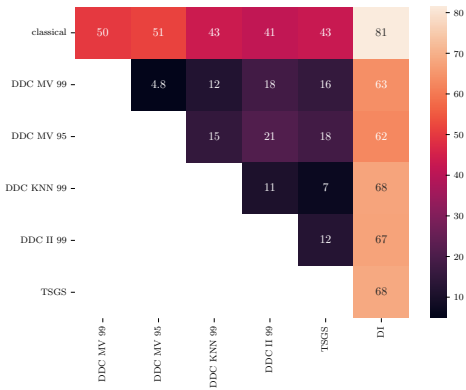


Figure 6: Relative spectral difference (in percentages) between estimated covariance matrices of the 30 features of sklearn’s Breast Cancer.

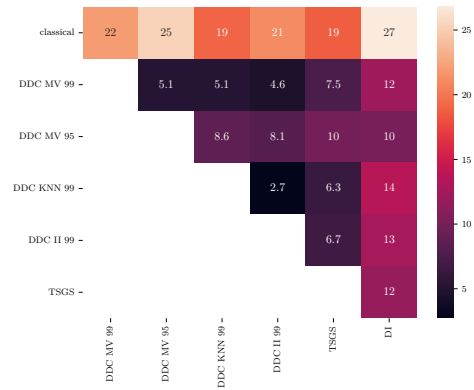


Figure 7: Relative spectral difference (in percentages) between estimated covariance matrices of the 13 features of sklearn’s Wine dataset.

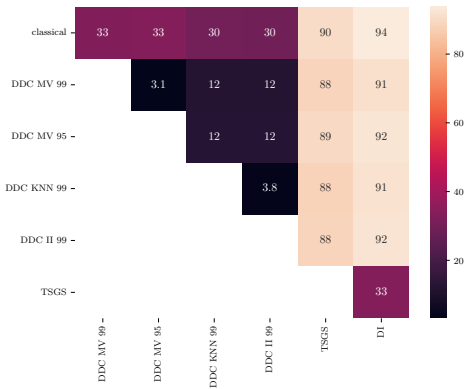


Figure 8: Relative spectral difference (in percentages) between estimated covariance matrices of the 11 features of the R camera dataset.

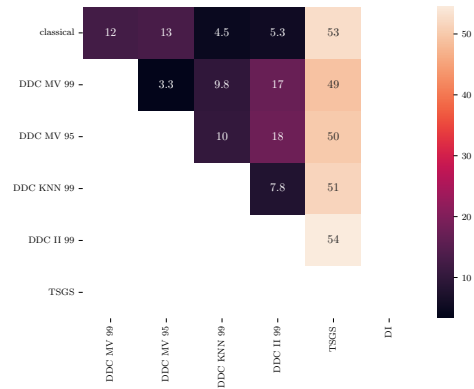


Figure 9: DI fails on ATTEND since the covariance matrix is approximately low rank. The dataset has only 8 features and the effective rank of its covariance matrix is below 2.

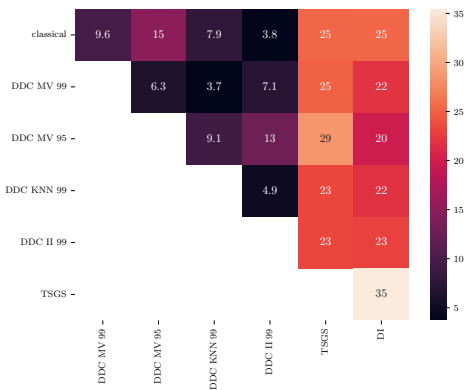


Figure 10: Relative spectral difference (in percentages) between estimated covariance matrices of the 11 features of the Woolridge Barium dataset.

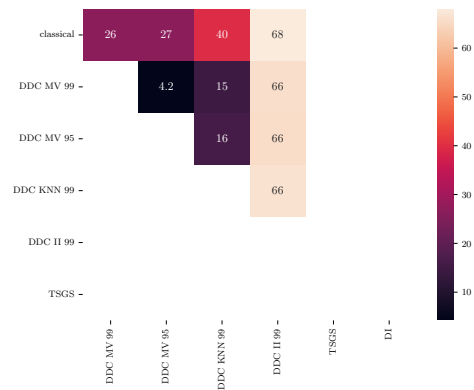


Figure 11: Woolridge’s CEOSAL dataset fails both TSGS and DI with its dimension of 13 and effective rank of around 2.5.



Table 8: Same table on the Abalone dataset, contaminated with a Gauss contamination.

CONTAMINATION RATE	TAIL CUT				DDC 99%				DDC 90%			
	$\hat{\delta}$	STD	$\hat{\varepsilon}$	STD	$\hat{\delta}$	STD	$\hat{\varepsilon}$	STD	$\hat{\delta}$	STD	$\hat{\varepsilon}$	STD
0.1%	69.5	0.001	0.016	0.010	98.0	0.013	0.059	0.009	93.2	0.019	0.056	0.009
1%	68.9	0.004	0.162	0.029	97.7	0.044	0.570	0.040	92.6	0.075	0.545	0.042
5%	66.2	0.028	0.852	0.055	93.5	0.058	2.86	0.045	89.8	0.119	2.73	0.050
10%	62.8	0.012	1.80	0.072	88.8	0.047	5.84	0.089	85.9	0.111	5.56	0.100
20%	55.9	0.008	3.95	0.088	79.6	0.044	12.5	0.098	77.7	0.123	11.6	0.103
30%	49.0	0.003	6.62	0.093	68.0	0.553	21.3	0.892	66.8	0.746	19.5	0.662

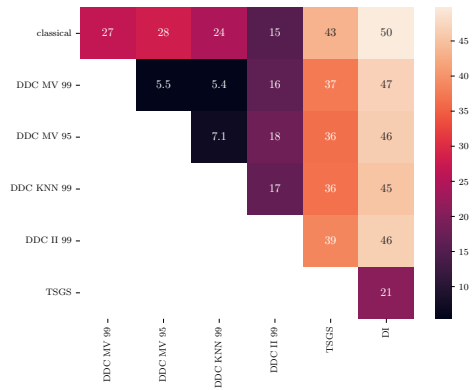


Figure 12: Relative spectral difference (in percentages) between estimated covariance matrices of the 13 features of Woolridge's INTDEF dataset.

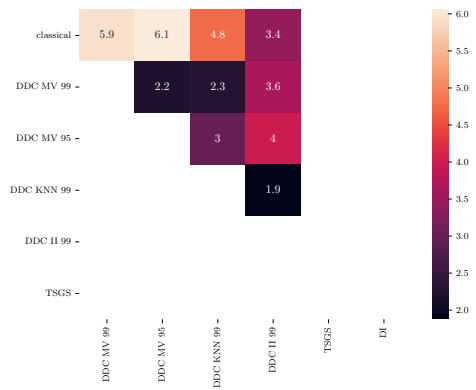


Figure 13: Relative spectral difference (in percentages) between estimated covariance matrices of SP500 stock returns over 2021 and 2022. On high-dimensional data, DDC II loses accuracy as compared to our other procedures DDC-MV and DDC KNN, mainly because IterativeImputer does not scale well with dimension.

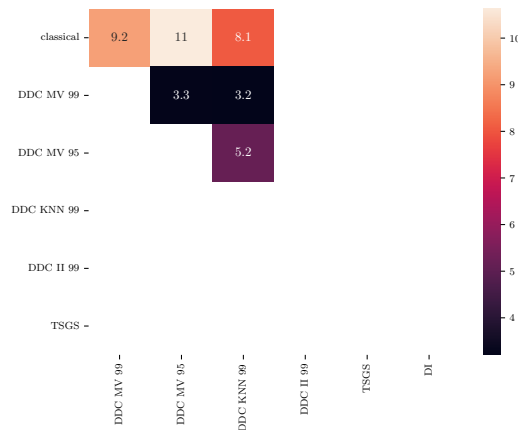


Figure 14: Relative spectral difference (in percentages) between estimated covariance matrices of NASDAQ stock returns over 2021 and 2022. Here, DDC II fails due to out-of-memory errors.